REGULATORY INFORMATION DISTRIBUTION SYSTEM (RIDS)

ACCESSION NBR:7812270178 DOC.DATE: 78/12/20 NOTARIZED: ~~NO~~ YES DOCKET #
FACIL:50-315 DONALD C COOK #1, INDIANA & MICHIGAN ELECTRIC CO. 05000315
50-316 DONALD C COOK #2, INDIANA & MICHIGAN ELECTRIC CO. 05000316
AUTH.NAME AUTHOR AFFILIATION
TILLINGHAST,J. IN & MI PWR
RECIP.NAME RECIPIENT AFFILIATION
DENTON,H.R. OFFICE OF NUCLEAR REACTOR REGULATION

SUBJECT: Forwards rept entitled "Hydraulic Model Investigation of Vortexing & Swirl within a Reactor Containment Recirculation Sump," dtd 780930.

DISTRIBUTION CODE: A001S COPIES RECEIVED:LTR 1 ENCL 40 SIZE: 2
TITLE: GENERAL DISTRIBUTION FOR AFTER ISSUANCE OF OPERATING LIC

NOTES: I+E - 3cys ALL MATL

	RECIPIENT ID CODE/NAME	COPIES LTTR	COPIES ENCL	RECIPIENT ID CODE/NAME	COPIES LTTR	COPIES ENCL
ACTION:	05 BC ORB#1	7	7			
INTERNAL:	01 REG FILE	1	1	02 NRC PDR	1	1
	12 I&E	2	2	14 HANAUER	1	1
	15 CORE PERF BR	1	1	16 AD SYS/PROJ	1	1
	17 ENGR BR	1	1	18 REAC SFTY BR	1	1
	19 PLANT SYS BR	1	1	20 EEB	1	1
	21 EFLT TRT SYS	1	1	22 BRINKMAN	1	1
EXTERNAL:	03 LPDR	1	1	04 NSIC	1	1
	23 ACRS	16	16			

DEC 29 1978

MA 2

GD

TOTAL NUMBER OF COPIES REQUIRED: LTTR 38 ENCL 38

REGULATORY DOCKET FILE COPY

INDIANA & MICHIGAN POWER COMPANY

P. O. BOX 18
BOWLING GREEN STATION
NEW YORK, N. Y. 10004

December 20, 1978
AEP:NRC: 00112

Donald C. Cook Nuclear Plant Unit Nos. 1 and 2
Docket Nos. 50-315 and 50-316
License DPR Nos. 58 and 74

Mr. Harold R. Denton, Director
Office of Nuclear Reactor Regulation
U.S. Nuclear Regulatory Commission
Washington, D. C. 20555

Dear Mr. Denton:

Enclosed please find forty (40) copies of the Alden Research Laboratory (ARL) report entitled, "Hydraulic Model Investigation of Vortexing and Swirl Within a Reactor Containment Recirculation Sump; Donald C. Cook Nuclear Power Station," September, 1978.

This report is submitted in fulfillment of Condition (3)(h) to the Operating License for the Unit No. 2 of the Cook Nuclear Plant. As the information contained in the subject ARL report is equally applicable to both units of the Cook Nuclear Plant, AEPSC requests that the report be placed on both Docket Nos. 50-315 and 50-316.

The subject report is being submitted at the request of the NRC staff and provides experimental verification of the adequacy of a previously reviewed and approved sump design. In light of the above, AEPSC interprets 10 CFR 170.22 as requiring that no fee accompany this submittal. (Reference: 10 CFR Part 170.22, footnote (2).)

Very truly yours,

John Tillinghast
Vice President

JT:em

Sworn and subscribed to before me
this 20th day of December, 1978 in
New York County, New York

William J. Prochaska
Notary Public

WILLIAM J. PROCHASKA
Notary Public, State of New York
No. 43-4636590
Qualified in Richmond County
Certificate filed in New York County
Commission Expires March 30, 1980

cc: (attached)

7812270178

A001
S
1/40

cc: R. C. Callen
G. Charnoff
P. W. Steketee
R. J. Vollen
R. Walsh
D. V. Shaller - Bridgman
R. W. Jurgensen

HYDRAULIC MODEL INVESTIGATION OF VORTEXING AND SWIRL WITHIN A REACTOR CONTAINMENT RECIRCULATION SUMP

DONALD C. COOK NUCLEAR POWER STATION

M. Padmanabhan

Research Sponsored by
American Electric Power Service Corporation

George E. Hecker, Director

ALDEN RESEARCH LABORATORY
WORCESTER POLYTECHNIC INSTITUTE
HOLDEN, MASSACHUSETTS 01520

September 1978

Printed at ARL - November 1978

ABSTRACT

American Electric Power Service Corporation authorized the Alden Research Laboratory (ARL) to conduct extensive hydraulic model testing of the Reactor Containment Sump of the Donald C. Cook Nuclear Power Plant, Units 1 and 2.

The main purpose of the model study was to verify that the reactor containment sump would perform satisfactorily without the development of any severe vortices or other flow irregularities that could affect the operation of the pumps in the Emergency Core Cooling System (ECCS) during its recirculation mode.

A model based on Froude similarity was designed and constructed to a scale of 1:2.5 to include the sump and the surrounding area of the containment building with all the structures that could influence the approach flow. Tests incorporating various possible flow and pump combinations under different possible restrictions, such as screen blockage, were undertaken. It was determined that the original design of the sump should be modified to reduce excessive swirl in the suction pipes under certain blockage conditions. A revised design incorporating fine mesh screens at the sump entrance was developed, and this design gave satisfactory performance under all possible operating conditions. Evaluation of inlet loss coefficients under different flow conditions was also performed in order to verify the available net positive suction head ($NPSH_{AV}$) of the pumps.

Detailed studies on possible scale effects of modeling vortices were conducted before projecting to prototype performance and recommending design modifications. This involved higher temperature and higher velocity tests in the model.

TABLE OF CONTENTS

INTRODUCTION

The reactor containment buildings of the Donald C. Cook Nuclear Power Station, Units 1 and 2, are provided with emergency core cooling systems (ECCS) designed to cool the shutdown reactor cores and the containments in the event of a loss of coolant accident (LOCA). The ECCS injects water to maintain core cooling and, initially, the water for this is drawn from the refueling water storage tank (RWST). When the water level in this tank is depleted to a predetermined level, the ECCS is switched from injection to recirculation mode. At this point, water is drawn from the containment recirculation sump containing water drained from the break, water from the ice condenser meltdown, and water from the containment spray system. The approach flow to the sump is affected by the equipments and appurtenant structures in the flow path. The water level, the pump discharges, and the water temperature could vary over a wide range during the recirculation mode, which lasts for an extended period of time to provide sufficient heat removal. It is very important that no adverse flow conditions that could affect performance of the pumps exist within the sump or the suction pipes. It is crucial that no air entraining vortices are formed and that the total intake losses are of a magnitude such that required NPSH of the pumps are satisfied.

The Alden Research Laboratory (ARL) was authorized by American Electric Power Service Corporation (AEPSC) to construct and test a model of the Donald C. Cook Nuclear Power Station containment recirculation sump with the object of investigating any free surface vortex formation or other undesirable flow conditions that could adversely affect the performance of the Residual Heat Removal (RHR) and Containment Spray Pumps (CTS), and Safety Injection (SI) Pumps of the Emergency Core Cooling Water System (ECCS) in the recirculation mode. Operating conditions involving a wide range of various possible approach flow distributions, water depths, water temperatures, screen blockage effects, and pump operating combinations were to be tested in the model. If potentially undesirable

flow conditions occurred, modifications in the sump configuration were to be developed. Factors subject to careful investigation in the model study were air entrainment due to vortexing, suction of entrapped air, swirl in the suction pipes, and the inlet losses at the sump. The scale effects on vortices, similarity of screen behavior, and means of extrapolating model results to prototype conditions were examined towards establishing conclusions of the study.

This report presents a description of the prototype and model, and summarizes conditions investigated, model construction, similitude considerations, test procedures, instrumentation, interpretation of results, and conclusions.

PROTOTYPE DESCRIPTION

Reactor Building

The reactor building is circular in plan as shown in Figure 1, with two concentric outer walls; namely, the crane wall and the containment wall, with inner radii of 41.5 ft and 57.5 ft, respectively. The steam generators, reactor coolant pumps, containment cleanup filter units, and the connected accessories are all located in the portion between the reactor chamber and the crane wall, as seen in Figure 1. The annular portion between the crane and containment walls accommodated the various pipes, valves, air ducts, and cables for various operating systems such as blowdown, cooling water, ventilation, and liquid waste recycling.

The Containment Recirculation Sump

The Containment Recirculation sump is located close to the crane wall between the steam generator number 2 and reactor coolant pump number 2 (extending from bearing 120 to 150 degrees approximately), as marked in Figure 1. The sump is more or less rectangular in plan, about 18 ft long and 10.5 ft wide, with the crane wall dividing it into two portions.

Flow would enter the upstream portion through stainless steel gratings provided at the entrance, flow down and under the crane wall, and finally enter the suction pipes. Figure 2 shows the sump details. As seen in this figure, the upstream portion would have a free surface while the downstream portion would be under pressure. The sump floor is at EL 591 ft 1 inch, whereas the building floor is at EL 598 ft 9-3/8 inches.

The top slab of the downstream portion of the sump is provided with a single air vent pipe running upward through the crane wall. The average approach velocity upstream of the grating would be about 0.34 fps at the minimum submergence (EL 602 ft 10 inches).

The two outlet pipes are 18 inches in diameter (Sch. 40), and are provided with bellmouth entrances and 24 inch diameter guard pipes. The suction pipes ran downward at an inclination of 13° 34' to horizontal, as shown in Figure 2. The center of the pipe entrance is at EL 595 ft 6 inches, and each pipe is connected to a valve at EL 589 ft 9 inches. A perforated plate, 1/8 inches thick with 1/4 inch diameter holes, is placed horizontally in the downstream portion of the sump just below the bottom of the bellmouth (at EL 593 ft 8-3/4 inches) to act as a fine screen.

As indicated in Figure 1, a lower sump, rectangular in plan (about 2 ft 4 inches by 4 ft 10 inches), and 7 ft 8-3/8 inches deep, is provided adjacent to the main containment sump to allow for proper drainage in normal conditions. This sump is connected to the main containment sump by an 8 inch diameter pipe.

Operating Cases for Tests

The discharge and submergence conditions at the sump would change with the different operating sequences from the instant of a LOCA. The following system operations were considered important in investigating the hydraulic performance of the sump:

1. 9500 gpm through one suction pipe - This simulates the runout condition of one ECCS train upon complete failure of the other train.

2. 7700 gpm per suction pipe, both pipes operating - This simulates the runout condition of ECCS pumps with both trains operating.

3. 9500 gpm through one pipe and 3600 gpm through the other - Same as case 1 except that the containment spray pump from the other train is at runout flow-rate.

Should a LOCA occur, the ECCS pumps, which are aligned to the refueling water storage tank (RWST), would inject 350,000 gallons of borated water into the primary loop before the recirculation sump is used. One train of ECCS pumps would be switched to the recirculation sump when the water level in the RWST reaches a predetermined low level, the time for this being about 10 minutes after the start of ECCS. The water level in the sump at this point is expected to be at EL 602 ft 10 inches. (This is a revised level, changed from the original value of EL 599 ft 5 inches).

It is not until the RWST reaches the lowest level that the second train of ECCS pumps would be switched to the recirculation sump. At this time, the entire 350,000 gallons would have been pumped into the sump via the primary loop. Even at worst conditions, allowing a non-usable volume of

128,000 gallons, the active containment sump would have been filled to EL 606 ft (for earlier testing, this level was assumed to be EL 602 ft 10 inches, as the exact value was not available at that time). If credit were taken for ice meltdown, this elevation would be 611 ft 8 inches.

Table 1 summarizes the system operations, each of which, for convenience, will be identified by the case number hereafter in this report. The water temperature of the breakflow, which would be collected in the sump, could be as high as 190°F. A high containment pressure of 3.0 psig would be possible.

ADVERSE FLOW CONDITIONS TO BE INVESTIGATED

The following are some of the likely flow conditions in a containment recirculation sump which could cause poor pump performance and hence were investigated during the model study.

1. Entrained Air - Air entrainment in the suction pipes could be due to air entraining vortices existing in the sump, due to suction of air entrapped below top cover plates in a submerged sump, or due to any other specific reason. It is established that even a low air concentration in the suction pipes, such as 3 to 5%, could lower the efficiency of the pump considerably (1). Hence, air entrainment is recognized as a major flow condition in the sump to be examined.

   Air entraining vortices (Types 5 or 6 of ARL classification, Figure 3), are not acceptable. However, due to scale effects in a Froudian model, it is possible that a Type 3 or 4 vortex in the model could represent a Type 5 or 6 in the prototype. It is important to demonstrate that scale effects are negligible or a suitable method of predicting prototype performance is used. The ARL uses a special high temperature-high flow test procedure to establish this aspect, apart from using the "Equal Velocity Rule" described in the subsequent sections.

2. Swirling Flow - The various possible approach flow patterns, together with possible vortexing, could induce considerable swirl in suction pipes and this is undesirable for the pumps. Excessive swirl could cause a fluctuating loading on the impeller, and could also affect the intake losses and thereby the available NPSH for the pumps. Measurement of swirl is accomplished in the model using a vortimeter in the suction pipe. It has not been well established what degree of swirl is allowable. Hence, to be conservative, it is desirable to eliminate or suppress swirl to the extent possible.

3. Losses Leading to Insufficient NPSH - A poorly designed sump could result in large intake losses. Intake losses caused by screens, poor entrance conditions, vortex suppression devices, etc., may add up to a value such that the required NPSH of the pump is not satisfied. The water temperature could also affect the available NPSH due to vapor pressure variations. The inlet losses are difficult to calculate theoretically, and model tests give a much more reliable value of inlet losses. With the derived values of the inlet losses, the NPSH available should be checked by recalculations.

The pipeline pressure gradient for a particular test was measured using photographs of the water columns connected to gradeline taps. An average friction gradient line was obtained from the photograph. The loss coefficients were determined using a common procedure (2) by extrapolating the measured pipeline gradient to the inlet and computing the head loss, h_L, as

$$h_L = \Delta h - u^2/2g \qquad (1)$$

where Δh is the head loss between the containment water surface (at a point outside the sump) and the extrapolated pressure gradeline at the pipe inlet. The loss coefficient, C_L, was defined as:

$$C_L = \frac{h_L}{u^2/2g} \qquad (2)$$

where $u^2/2g$ represents the velocity head in the pipe. Figure 4 shows a typical evaluation of C_L from pressure gradient data.

SIMILITUDE

The study of dynamically similar fluid motions forms the basis for the design of models and the interpretation of experimental data. The basic concept of dynamic similarity may be stated as the requirement that two systems with geometrically similar boundaries have geometrically similar flow patterns at corresponding instants of time (3). Thus, all individual forces acting on corresponding fluid elements of mass must have the same ratios in the two systems.

The condition required for complete similitude may be developed from Newton's second law of motion:

$$F_i = F_p + F_g + F_v + F_t \qquad (3)$$

where

F_i = inertia force, defined as mass, M, times the acceleration, a

F_p = pressure force connected with or resulting from the motion

F_g = gravitational force

F_v = viscous force

F_t = force due to surface tension

Additional forces may be relevant under special circumstances, such as fluid compression, magnetic or Coriolis forces, but these had no influence on this study and were, therefore, not considered in the following development.

Equation (3) can be made dimensionless by dividing all the terms by F_i. Two systems which are geometrically similar are dynamically similar if both satisfy the dimensionless form of the equation of motion, Equation (3). We may write each of the forces on the right side of Equation (3) as:

F_p = net pressure x area = $\alpha_1 \Delta p L^2$

F_g = specific weight x volume = $\alpha_2 \gamma L^3$

F_v = shear stress x area = $\alpha_3 \mu \Delta u/\Delta y$ x area = $\alpha_3 \mu u L$

F_t = surface tension x length = $\alpha_4 \sigma L$

F_i = density x volume x acceleration = $\alpha_5 \rho L^3 u^2/L = \alpha_5 \rho u^2 L^2$

where

α_1, α_2, etc. = proportionality factors

L = representative linear dimension

Δp = net pressure

γ = specific weight

μ = dynamic viscosity

σ = surface tension

ρ = density

u = representative velocity

Substituting the above terms in Equation (3) and making it dimensionless by dividing the inertial force, we obtain

$$\frac{\alpha_1}{\alpha_5} E^{-2} + \frac{\alpha_2}{\alpha_5} F^{-2} + \frac{\alpha_3}{\alpha_5} R^{-1} + \frac{\alpha_4}{\alpha_5} W^{-2} = 1 \qquad (4)$$

where

$$E = \frac{u}{\sqrt{\Delta p/\rho}} = \text{Euler number} \propto \frac{\text{Inertia Force}}{\text{Pressure Force}}$$

$$F = \frac{u}{\sqrt{gL}} = \text{Froude number} \propto \frac{\text{Inertia Force}}{\text{Pressure Force}}$$

$$R = \frac{u\,L}{\mu/\rho} = \text{Reynolds number} \propto \frac{\text{Inertia Force}}{\text{Viscous Force}}$$

$$W = \frac{u}{\sqrt{\sigma/\rho L}} = \text{Weber number} \propto \frac{\text{Inertia Force}}{\text{Surface Tension Force}}$$

Since the proportionality factors, α, are the same in model and prototype, complete dynamic similarity is achieved if all the dimensionless groups, E, F, R, and W, have the same values in model and prototype. In practice, this is difficult to achieve. For example, to have the values of F and R the same requires either a 1:1 "model" or a fluid of very low kinematic viscosity in the reduced scale model. Hence, the accepted approach is to select the predominant force and design the model according to the appropriate dimensionless group. The influence of other forces would be secondary and are called scale effects (2, 3).

Froude Scaling

Models involving a free surface are constructed and operated using Froude similarity since the flow process is controlled by gravity and inertia forces. The Froude number, representing the ratio of inertia to gravitational force,

$$F = u/\sqrt{gs} \tag{5}$$

where

u = average velocity in the pipe
g = gravitational acceleration
s = submergence

was, therefore, made equal in model and prototype

$$F_r = F_m/F_p = 1 \tag{6}$$

where m, p, and r denote model, prototype, and ratio between model and prototype, respectively.

In modeling of an intake sump to study the formation of vortices, it is important to select a reasonably large geometric scale to achieve large Reynolds numbers and to reproduce the curved flow pattern in the vicinity of the intake (4). A geometric scale of $L_r = L_m/L_p = 1/2.5$ was chosen for the model, where L refers to length. At higher Reynolds number, an asymptotic behavior of energy loss coefficients with Reynolds number is usually observed in similar flows (2). Hence, with $F_r = 1$, the basic Froudian scaling criterion, the Euler numbers, E, will be equal in model and prototype. This implies that flow patterns and loss coefficients are equal in model and prototype. From Equation (6), using $s_r = L_r$, the velocity, discharge, and time scales were:

$$u_r = L_r^{0.5} \tag{7}$$

$$Q_r = L_r^{2}\, u_r = L_r^{2.5} \tag{8}$$

$$t_r = L_r^{0.5} \tag{9}$$

Similarity of Vortex Motion

The fluid motions involving vortex formation in the sumps of low head pump intakes have been studied by several investigators (1, 4, 5, 6). Anwar (4) has shown by principles of dimensional analysis that the dynamic similarity of fluid motion in an intake is governed by the dimensionless parameters given by:

$$\frac{4Q}{u_\theta d^2}, \quad \frac{u}{\sqrt{2gs}}, \quad \frac{Q}{\nu s}, \text{ and } \frac{d}{2s}$$

where

Q = discharge through the inlet

u_θ = tangential velocity at a radius equal to that of the outlet pipe

d = diameter of the outlet pipe

Surface tension effects were neglected in this analysis. The influence of viscous effects was defined by the parameter $Q/(\nu s)$, known as a radial Reynolds number, R_R.

For similarity between the dimensions of a vortex of types up to and including the narrow air-core type, it was shown that the influence of R_R becomes negligible if $Q/(\nu s)$ was greater than 10^3. As strong air-core type vortices, if present in the model, would have to be eliminated by modified sump design, the main concern for interpretation of prototype performance based on the model performance would be on the similarity of weaker vortices, such as surface dimples and dye-cores. For the prototype of the present study, the values of R_R for the operating temperature ranges of 80°F to 190°F ranged from 0.48×10^5 to 9.5×10^5. The value of R_R for the 1:2.5 model was always greater than 10^3 for water temperature of 40°F and above. Referring to Daggett and Keulegan (5), the viscous effects on vortexing phenomenon would be negligible if the

Reynolds number, $R = ud/\nu$, is greater than 3.2×10^4. For a 1:2.5 model, the minimum value of R in this study would be 1.6×10^5. Thus, viscous forces might be expected to have only a secondary role in the present study. If so, dynamic similarity is obtained by equalizing the parameters $4Q/u_\theta d^2$, $u/\sqrt{2gs}$, and d/2s in model and prototype. A Froudian model would satisfy this condition, provided the curved approach flow pattern in the vicinity of the sump is properly simulated, which requires a large size model. A 1:2.5 model satisfied this requirement (4). However, potential scale effects due to viscous forces in the present model were investigated by special testing procedures (7), which will be referred to in this report as high temperature-high velocity tests and discussed subsequently.

Scale Effects on Vortices

Viscous and surface tension forces could influence the formation and strength of vortices (4, 5). The relative magnitude of these forces on the fluid inertia force is reflected in the Reynolds and Weber numbers, respectively, which are defined as:

$$R = u\, d/\nu \tag{10}$$

$$W = \frac{u}{(\sigma/\rho s)^{1/2}} \tag{11}$$

It was important for this study to ascertain any deviations in similitude attributable to viscous and surface tension forces in the interpretation of model results to prototype conditions. Surface tension effects were considered negligible inasmuch as strong vortices were unacceptable, and the free surface was essentially flat for all final tests. Moreover, an investigation using liquids of the same viscosity but different surface tension coefficients ($\sigma = 4.9 \times 10^{-3}$ lb/ft to 1.6×10^{-3} lb/ft) showed practically no effect of surface tension forces on the vortex flow (5). The vortex severity, S, is therefore mainly a function of the Froude number, but could also be influenced by the Reynolds number.

$$S = S\ (F,\ R) \qquad (12)$$

The possible scale effect due to different Reynolds number in the model and prototype was ascertained before predicting vortex types for the prototype based on model observations. For this projection, technique, and for consistent observations, it is convenient to classify the free surface vortices from a swirl to an air core type vortex, as shown in Figure 3.

Equal Velocity Rule

To compensate for the excessive viscous energy dissipation and consequent less intense model vortex, various investigators have proposed increasing the model flow and therefore the velocity keeping the submergence constant. Operating the model at the prototype inlet velocity (pipe velocity) is believed by many researchers to achieve the desired results (1). This is often referred to as Equal Velocity rule and is considered to give conservative predictions of prototype performance. The test procedure for the present study would incorporate testing at prototype velocities in the pipe, in accordance to this rule.

High Temperature-High Velocity Testing

Figure 5 illustrates the method used to investigate scale effects and predict vortex types in the prototype based on model results (7). The ordinate, F_r, is the ratio of model to prototype Froude number while the abscissa is the inlet pipe Reynolds number, R. Assume the model to operate at flow less than Froude scaling ($F_r < 1$) at point a_1. By increasing the discharge in the model while keeping the same submergence and temperature, F_r and R are increased corresponding to a point, a_N, where a vortex of type N was first observed. The model Reynolds number can also be changed by varying the kinematic viscosity with temperature changes, and similar tests performed to locate b_N, another

point on the locus of type N vortices. Extrapolation of the line of constant vortex strength of type N can be made to a prototype Reynolds number at the proper Froude number ($F_r = 1$), point p_N. The locus could indicate any expedient measure of vortex severity. Any scale effects due to viscous forces would be evaluated and taken into account by such a projection procedure. The high temperature-high velocity tests could also be used in the similar fashion for projecting the inlet loss coefficients (from the pressure gradient measurements) and the swirl severities (from vortimeter readings) over a wide range of Reynolds and Froude numbers.

The inlet loss coefficient, C_L (alternately, the coefficient of discharge), may be affected by circulation (5) and hence could also form a measure of vortex severity. In the absence of circulation, this loss coefficient would not show any increase with R, whereas increasing circulation associated with vortices could affect this trend. Hence, measurements of pressure gradient in the pipe and evaluation of the loss coefficients could help judging the vortex severity.

The effect of circulation on the coefficient of discharge has been previously investigated (5). The angular momentum of the flow due to the swirl and vorticity is approximately conserved through the inlet since the tangential shear is small (6). The angular velocity of the transmitted swirl could be measured using a cross vane vortimeter. From the number of vortimeter rotations per unit of time, n, a representative measure of the tangential velocity, u_t, could be obtained as:

$$u_t = \pi n\, d \tag{13}$$

d being the pipe diameter. The values of u_t may be used to compare the vortex severity. An angle of indicated swirl may be defined (6) as:

$$\theta = \tan^{-1} u_t/u \tag{14}$$

The classification of vortex type by number as explained in Figure 3 could be correlated with the angular velocity measurements using the cross vane vortimeter. This allows identification of the average vortex severity in a timely and consistent manner, especially when the vortices are not steady. However, when more than one vortex is present at an inlet, the interaction between vortex cores rotating in opposite directions could give vortimeter readings not appropriate to the observed vortex type. However, the vortimeter reading would still provide an indication of the total induced swirl in the pipe.

MODEL DESCRIPTION AND INSTRUMENTATION

General Layout

A physical model of the containment sump and a portion of the reactor building forming the approach to the sump were constructed to a geometric scale of approximately 1:2.5 on an elevated platform, as shown in Photograph 1. The portion of the containment building modeled is marked in Figure 1.

The model was operated based on Froude's Law. The model was essentially a steel tank formed as a segment of a circle in plan with a radius of about 17.5 ft. The model walls were about 6 ft high from the model floor, which was elevated by about 4 ft from the laboratory building floor. All the appurtenant structures in the vicinity of the sump that could influence the approach flow were simulated up to the maximum water level. The model floor and walls were constructed of steel plates with necessary supports and bracings. The walls at the depressed sump portion and a portion of the wall above it were made of plexiglass to facilitate observation and photography. The top cover plates of the sump were also made of plexiglass. The lower sump adjacent to the main containment sump (Figure 1) was also modeled.

Piping Details

Two 7 inch diameter (6.75 inch ID) pipes about 13 ft long sloping down at an angle of 13° 34' to horizontal formed the suction pipes (Photograph 2). Both the pipes were provided with a plexiglass removable portion for inserting a vortimeter and for observational purposes. The portion of the suction pipes beyond the inclined portion was not modeled. Figures 6 and 7 show the pipe layout, and the suction pipes will be identified in this report by the numbers indicated in Figure 7. The pipes were about 13 ft long outside the model boundary and were connected to 12 inch horizontal pipes using expansion pieces. The two 12 inch pipes were ultimately joined to a 16 inch pipe with a Y-joint. The 12 inch pipes were provided with calibrated orifice plates for flow measurement. The 16 inch pipe formed the suction pipe to a 40 HP main supply pump which delivered the water back to the model, forming a closed loop system. The closed loop system enabled easy water level settings and also helped in maintaining the water quality. For filling and emptying the model tank at the beginning and end of testing, and also for water level adjustments, a separate 3 inch diameter pipe loop with a small 3 HP pump was used. The water volume in the model tank could thus be increased or decreased by pumping from or into the laboratory building sump. It was also possible to heat the water in the model tank by recirculating it through a 100 HP boiler using a separate 6 inch line and a 3 HP pump. The water in the laboratory sump was cleaned continuously using a sand filter to ensure good water quality. The pipes were provided with air bleeds at high points to remove air during filling of the model.

The inclined portions of each of the two suction pipes were provided with ten pressure taps, one pipe diameter apart; the first one being at 13 diameters from the bellmouth entrance (Figure 7). These pressure taps were connected to a manometer board. Separate piezometer tubings connected to four different openings in the model floor enabled the pressure

gradient measurements to be related to the water level inside and outside of the sump gratings and crane wall. The water levels in the tubes were measured with a moving point gage with vernier (to 0.001 ft), and the water levels in the tubes of the manometer board were measured using photographic techniques.

Model Operation

The model tank was filled to the desired level using the 3 inch pipe loop with clean water from the laboratory sump. The main pump was then started and the flow in each pipe could be adjusted with the valves in the 12 inch lines, as well as the valve in the delivery line, to a desired flow as indicated by pressure drop across orifice meter. The water level in the model could be adjusted, if required, by adding or taking out water from the laboratory sump. The water in the model tank could be recirculated through the boiler if heating was necessary.

Screens and Gratings

The sump portion of the model was provided with a vertical trashrack grating (1 inch deep bars at 15/16 inch c/c) through which the approach flow entered. As the head loss through this grating would be negligibly small based on calculations (less than 0.01 inch), the grating was not modeled to scale, but a grating with same geometric parameters as in the prototype was used in the model. However, the framework supporting the grating was modeled to scale, being of larger dimensions.

The horizontal perforated plate was modeled to simulate head losses across the plate. Consequently, a plate with smaller holes but with same percentage open area was chosen in the model. The prototype plate of 1/8 inch thick, 1/4 inch diameter holes at 3/8 inches c/c was modeled with a plate of 1/16 inches thick, 1/8 inch diameter holes at 3/16 inches c/c.

It was later recommended that a fine screen be placed behind the grating and the perforated plate be removed. The prototype screen was to be selected to give a same loss coefficient as the prototype. A 0.25 inch mesh, 1/16 inch wire, fine screen was used in the model for which a pressure loss versus screen Reynolds number curve was available from an earlier investigation at ARL (8).

Observation Techniques

For the identification and classification of vortices, visual and photographic observations were made with the assistance of tracers such as dye and cotton balls. Swirl in the inlets was measured using a crossed vane vortimeter which could be fixed inside pipe 1 or 2 (Photograph 3).

TEST PROCEDURE

Tests were conducted in three phases as indicated below.

Phase 1 - Preliminary test series - testing of numerous combinations of pump operations, discharges, water levels, and farfield blockages at normal ambient laboratory temperature - selection of a few critical combinations - determination of inlet loss coefficients.

Phase 2 - Retesting critical combinations at scaled and prototype pipe velocities with grating blockage and perforated plate blockage - vortimeter readings for critical combinations - appraisal of the sump performance based on vortex severity, swirl severity, and entrance losses - evolving a revised sump design, as necessary.

Phase 3 - Retesting the selected revised sump configuration - detailed screen blockage tests - high temperature-high velocity tests - detailed inlet loss evaluation - conclusions on revised sump performance and recommendations.

A more detailed description of each of the testing phases follows. The minimum water level for Phase 2 was assumed to be EL 602 ft 10 inches for much of the earlier tests as exact values were not available at that time. However, this elevation made those results conservative as the actual minimum water level was determined to be EL 606 ft for Case 2.

Phase 1 - Test Series

Table 1 shows the details of five operating cases considered for the testing. Testing was done for both F_r = 1 and 1.58 (Froudian scaled and prototype velocities). Worst conditions for vortexing may be expected when maximum flow occurs at the lowest submergence. Various approach flow distributions were possible due to farfield obstructions and the location of breaks as indicated in Table 2. For the various combinations of five operating cases and two submergence depths, tests were conducted with various approach flow distributions in a sequence as indicated in Table 3 to select a few critical combinations based on swirl and vortexing. The inlet loss coefficients were evaluated for both the suction pipes with the water level corresponding to the minimum water level and with no blockage effects.

Phase 2 - Test Series

For the critical combinations derived from Phase 1 testing, tests to identify vortex severities due to grating blockage were first undertaken. A few blockage schemes were tried with minimum water level and for operating Case 2 with 50% of the grating area blocked (Figure 8). Blockages were produced with plywood strips placed on the grating. A worst scheme was chosen to be tested for all the six critical combinations selected. Vortimeter readings were noted to estimate swirl severities. As a second

step, detailed testing on the perforated plate blockage was undertaken by trying various combinations to effect up to 50% blockage (Figure 9). Few inlet loss measurements were taken. The last part of Phase 2 tests were the high temperature-high velocity tests (explained earlier in the section on Similitude). The water was heated to temperatures from 60°F to 165°F. For four different temperatures in this range, the Froude number ratio was varied from 0.8 to 1.58 by changing flow, keeping submergence to that of the worst operating case found from Phase 1 tests. The results of Phase 1 and 2 tests were used to decide the various possible changes on the location and design of the sump necessary and to select a revised sump design for further testing.

Phase 3 - Test Series

These tests constituted the final series of tests on a selected revised sump design to confirm the satisfactory performance of the sump. Extensive tests with different blockage schemes were done for different operating cases to identify a worst blockage scheme. Swirl measurements and vortex observations were conducted for this purpose for each run. The flow was varied from 0.5 to 2 times the Froude scaled value to obtain the inlet loss coefficients over a wide range of Reynolds number, keeping the submergence constant. Each of the five operating cases were tested at their corresponding minimum water levels to obtain data on types of vortices observed, vortimeter reading and inlet loss coefficients for both Froude scaled velocities and prototype velocities (F_r = 1 and 1.58) with and without screen blockage. At this point, the necessity of any additional design changes were ascertained and affected if found needed.

The worst screen blockage scheme, as indicated by extensive tests done in the earlier part of Phase 3 tests, was incorporated in tests. Vortex observations and swirl measurements were made for each setting. High temperature-high velocity tests and inlet loss measurements were made for a few runs to compare with the earlier findings. Final conclusions and recommendations were drawn from the results of Phase 3 tests.

RESULTS AND DISCUSSIONS

Phase 1 Tests

Preliminary tests indicated that the minimum water level in the sump should not be less than EL 602 ft 3 inches so that the necessary head over the curb to effect the needed inflow balancing the outflow from the sump was available. The revised value of the minimum water level given by AEPSC (EL 602 ft 10 inches), hence, was found sufficient.

Phase 1 tests, as per the test sequence indicated in Table 3, showed that for all the operating cases considered, the farfield obstructions affected the approach flow pattern and hence the positions of the eddies and surface dimples observed within the sump. But, no significant influence of these approach flow patterns on the severity of vortices or intensities of swirl were observed. Only unstable and intermittent surface dimples and eddies shed by the columns supporting the gratings were present inside the sump area. The maximum intensity of swirl corresponded to a swirl angle of about 5 degrees for operating Case 1 at its minimum water level of EL 602 ft 10 inches.

It was observed that the severity of vortexing and swirl intensities were always higher at the corresponding minimum water levels for all the operating cases. As a part of a preliminary testing, the inlet loss coefficient for pipe 2 over a Reynolds number range of 2.9 to 4.5 x 10^5 was evaluated for operating Cases 1 and 2 at the minimum water level of EL 602 ft 10 inches and was found to be about 0.20 on the average.

Phase 2 Tests

a. Grating Blockage Tests

Various grating blockage schemes, producing up to 50% blockage as shown in Figure 8, were tested for operating cases 1 and 2 at both Froudian and prototype velocities to identify a few schemes producing severe vortexing and/or swirl. Table 4 gives the details. For these tests,

the minimum water level for operating case 2 was set at EL 602 ft 10 inches (the actual value of this water level in the prototype would be EL 606 ft). As seen from Table 4, the blockage schemes 3 and 5 produced more intense vortexing and swirl. Photograph 4 shows the vortex activity inside the sump for blockage scheme 3 and operating case 2 at prototype velocities in suction pipes, (F_r = 1.58). The vortices were unstable, intermittent, and occasionally stronger and derived their energy mainly from eddies shed by the blockage. As shown in Figure 10, the vortices were mostly of Types 2 to 4 (ARL classification, Figure 3) for F_r = 1.58 and were less intense, types 1 to 2, at Froudian velocities, F_r = 1.

b. Perforated Plate Blockage Tests

For different grating blockages, various blockage schemes of the horizontal perforated plate (Figure 9) producing up to 50% blockage were tested for operating cases 1 and 2, again for both F_r = 1 and 1.58. Swirl angles of more than 10 degrees were indicated for some of the blockage schemes. For blockage scheme 4, the intense swirl produced a submerged air-core, as shown in Photograph 5, for F_r = 1.58. As the perforated plate was very close to the suction pipe entrance, the blockage of the plates in a certain scheme produced an undesirable approach flow pattern which generated the intense swirl. Table 5 summarizes the results of perforated plate blockage tests for F_r = 1.58. Even at the Froudian velocities, certain blockages produced swirling flow with swirl angles of about 8 to 9 degrees.

c. Changes in Sump Configuration

As there was no fine mesh vertical screen provided behind the grating, the horizontal perforated plate, with 1/4 inch holes, located behind the crane wall was meant to act as a fine mesh screen required to prevent fine debris entering the suction pipes. The results of phase 2 tests indicated that the likely blockage of the perforated plate produced swirling flow in the suction pipe with indicated swirl angles much greater than 5 degrees, which may be objectionable. Therefore, it was

decided to install vertical fine mesh screens behind the grating with openings less than 0.25 inches to replace the perforated plate. A screen of 1/16 inch wire and 4 meshes/inch was installed in the model just behind the vertical gratings and further testing was continued after this modification.

d. Air Venting Under Cover Plates

During phase 2 tests, it was noticed that the single air vent pipe provided at the left half of the sump on the top cover at EL 596 ft 9-1/4 inches downstream of crane wall was not efficient in removing all the air caught up beneath the top cover while the sump was filled up. A better venting system should be provided and recommendations would be made to this effect. Few air release valves were provided in the model to vent the trapped air. The present air vent pipe may be extended along the crane wall above the maximum water level to avoid water flow through this vent pipe which might interfere with its air venting ability. This change was not effected in the model, being not important.

e. High Temperature-High Flow Tests

To establish whether any scale effects due to viscous forces exist and to project the likely performance of the prototype based on vortexing and swirl, high temperature-high flow tests, as described earlier in this report, were undertaken. The model was run at operating case 2 with submergence corresponding to EL 602 ft 10 inches. Figures 11 and 12 show the results. Operating case 2 with water level at EL 612 ft 10 inches and with 50% screen blockages, was considered. The Froude number was varied by varying the flow through both suction pipes by equal proportions to give values of Froude number ratio, F_r, equal to 0.8, 1.0, 1.2, 1.4, 1.6, and 1.8 for each of the four temperatures tested; namely, 60, 95, 135, and 165°F. Table 6 gives the results of these tests. It could be seen that no observable changes in the vortex activity with Reynolds number existed for the same Froude number ratio

(Figure 11). The locus of the vortices of a given severity was more or less horizontal indicating no scale effects due to viscous effects. A prediction of vortex types in the prototype operating range under the same conditions would indicate only surface swirls and dimples and no vortices with any coherent cores. Figure 13 indicates the types and location of vortices for $F_r = 1.6$.

Figure 12 shows the vortimeter readings and it can be seen that swirl intensities were also free from any scale effects. In short, Figures 11 and 12 confirmed that practically no scale effects due to viscous forces were apparent. It may be noted that the revised minimum water level for operating case 2 was EL 606 ft and not EL 602 ft 10 inches. However, as the intent of the high temperature-high flow tests was to establish any scale effects, this difference was not of any importance. Phase 3 tests incorporated a retesting with correct water levels to identify the vortex types and to present the results valid for the final design. A few tests at higher temperatures (for operating case 1) were also undertaken under Phase 3 testing for the revised sump design and are reported in the next section.

Phase 3 Tests

a. Final Revised Sump Configuration

With the introduction of the vertical fine mesh screen, it became apparent that the horizontal perforated plate had little purpose in improving the flow within the sump. Further, the remote possibility of the blockage of holes in the perforated plate in spite of the vertical fine screen discouraged retaining the perforated plate. Consequently, it was decided to remove the perforated plate altogether. This was done in the model before phase 3 tests began. Photograph 6 shows the modified sump.

b. Retesting Screen Blockage

For various screen blockage schemes (Figure 8), retesting to provide final results on the revised sump performance at appropriate water levels for all the cases was undertaken and the results are included in Table 7. Figures 13 and 14 show the vortexing observed for operating cases 1 and 2 at their corresponding minimum water levels; namely, EL 602 ft 10 inches and 606 ft, respectively, and with 50% screen blockage (scheme 5). For operating case 1, the vortices were of type 1 to 2 for F_r = 1 and of type 1 to 3 for F_r = 1.58 (Photograph 7). No coherent core existed and the surface dimples were mostly eddies shed by grating supports and blockage pieces. For operating case 2, the water level was above top cover at EL 604 ft 11-3/4 ft and hence the free surface existed outside the screen and grating. As shown in Figure 14, the vortexing was outside the sump area and vortices of types 3 or less were observed. These vortices were highly intermittent, unstable, and no coherent core existed strong enough to go past the grating and screen which also acted as vortex suppressors. In fact, these vortices were imparted energy by unstationary eddies shed by the pipe connecting steam generator to reactor coolant pump. It was observed that an air venting arrangement would be necessary at the top cover to avoid air being trapped underneath. In the model, a row of 1/2 inch holes drilled on the cover was seen to vent the trapped air effectively.

The revised sump configuration was thus found to perform very well without causing any severe vortexing even at prototype velocities and with 50% screen blockage. The maximum indicated swirl angle was always less than 5 degrees for all the operating cases under the various screen blockage schemes tested, as seen from Table 7.

c. High Temperature-High Flow Tests for Revised Sump

Even though the high temperature-high flow tests performed under phase 2 testing were sufficient to prove that the scale effects were negligible in this large size model, it was decided to perform a few tests for the

revised final sump configuration to supplement the earlier findings. Tests were conducted to observe vortex severities for operating case 1 at its minimum water level for Froude's number ratios of 1.0, 1.6, 1.8, and 2.0 at temperatures of 66, 96, 138, and 164°F. Figure 15 and Table 8 show the details. It could be projected that the prototype sump would have only surface dimples and no coherent core type of vortices would be present. The final sump configuration is thus found satisfactory.

d. Inlet Loss Coefficients

Pressure gradient measurements were taken for the original sump configuration with the horizontal perforated plate for earlier tests. Pressure gradient data was obtained for different operating cases over a range of Reynolds numbers, 2.5 to 11 x 10^5, and the results are given in Table 9 and Figure 16. Most of the data were obtained for pipe 1. The data obtained for pipe 2 showed practically no significant differences in the value of C_L. Photograph 7 shows a typical hydraulic gradeline for pipe 1 obtained for operating case 2 with 50% screen blockage corresponding to scheme 3. Figure 16 shows the C_L versus R data for pipe 1 and it is seen that the average value of C_L is about 0.27. No Reynolds number effect on values of C_L was observed. For the revised sump configuration, the pressure gradient measurements were repeated and the results are included in Table 10 and Figure 17. The average value of C_L is about 0.24. The value of C_L indicates the total losses including the screen, grating, and entrance losses. The loss of head across the grating and screen was evaluated by separate tests and was found to be about 11.5 times the approach velocity head just upstream of the grating.

e. Tests at Other Higher Submergences

Few tests were conducted at higher submergences in the range of water levels corresponding to EL 602 ft 10 inches to EL 606 ft for operating cases 1a and 1b with 50% screen blockages (included in Table 7). These tests showed that the vortex severity and swirl intensities were less severe as the submergence was increased and hence a satisfactory sump performance at all operating discharges and corresponding submergences was found to exist.

f. Scaling of Screen Dimensions

The pressure loss coefficient to Reynolds number relationship of the model fine screen used in this study was available from an earlier investigation (8). Based on the similarity of pressure loss and velocity modifications, it would be appropriate in this case to use a screen of the same characteristics as the model fine screen. The effects of turbulence produced by the screens on the vortices were assumed to be negligible for this study. This is based on the fact that at low screen Reynolds numbers (on the order of 1000), the turbulent fluctuations and mean eddy size would be very small a few wire diameters away from the screen (3).

SUMMARY AND CONCLUSIONS

A 1:2.5 undistorted scale model of the Containment Recirculation Sump of the D.C. Cook Nuclear Power Station was tested to ensure that undesirable flow patterns that could result in a poor performance of the pumps in the Emergency Core Cooling System will not exist for the various operating conditions during the recirculation mode. Preliminary studies were undertaken to select a few critical flow combinations out of the many possible combinations of pump operating cases, water surface elevations, and discharges.

Further studies with grating and perforated plate blockages showed the existence of swirl and formation of submerged air core in the event of asymmetrical blockage of the horizontal perforated plate with prototype velocities in the pipe. Modifications in the sump design were developed and tested. The modified sump had a vertical fine mesh screen behind the vertical grating at the entrance to the sump. The horizontal perforated plate was completely removed. Better air-venting on the top cover plates was also recommended. The effect of possible scale effects on vortices in the model was ascertained using the results of high temperature-high flow tests. Table 11 shows a comparison of original and revised sump performance.

The essential findings of this hydraulic model study are itemized as follows:

1. As far as vortexing and swirl were concerned, the original D.C. Cook Containment sump was found to perform satisfactorily for all operating cases considered. Under the condition simulating blockage of horizontal perforated plate, swirl was observed in the suction pipes.

2. Intense swirl was generated by certain blockage configurations of the original perforated plate. The indicated swirl angle of the flow in the suction pipes under these conditions were more than 7 degrees. To improve the sump performance, it was found necessary to completely remove the perforated plate and to provide vertical fine mesh screens (0.063 inch wires; 4 meshes per inch) behind the vertical gratings at the sump entrance.

3. The modified sump produced no objectionable vortexing for all the operating conditions tested. The intensity of swirl was relatively low, with an indicated swirl angle in the suction pipes of about 4 degrees.

4. The minimum water level in the sump during the recirculation mode should not fall below EL 602 ft 3 inches so as to provide enough head over the curb (under possible 50% grating blockage) for effecting the necessary inflow to balance the outflow. The water level of EL 602 ft 10 inches is satisfactory.

5. A projection to the prototype performance, based on the results of the high temperature-high flow tests of the recommended design, showed that no objectionable vortexing problems would exist in the prototype. Only surface swirls, dimples, and surface eddies are expected inside the sump.

6. The inlet loss coefficients, C_L, for both the suction pipes were evaluated for a range of pipe Reynolds numbers, R. It was observed that no significant changes of C_L occurred within the wide range of R tested. The values of C_L for both the pipe inlets were in the range of 0.21 to 0.28 for a worst screen blockage system, including losses due to screens, racks, and gratings.

7. Some air entrappment underneath the two solid top covers was observed in the model. As entrapped air is undesirable, it is recommended that the top cover upstream of the crane wall may be provided with a number of holes of about 1/2 inch diameter. This would allow the air to escape as the water level rises in the sump. The single air vent pipe provided at the top cover outside the crane wall was found to be inadequate, and it is recommended that more such pipes be provided at various locations along the top cover.

REFERENCES

1. Denny, D.F., and Young, G.A.J., "The Prevention of Vortices and Swirl at Intakes," 7th General Meeting Transactions, IAHR, Lisbon, 1957.

2. Daily, J.W., and Harleman, D.R.F., Fluid Dynamics, Addison-Wesley Publishing Company, 1965.

3. Rouse, H., Handbook of Hydraulics, John Wiley & Sons, 1950.

4. Anwar, H.O., "Prevention of Vortices at Intakes," Water Power, p. 393, October 1968.

5. Daggett, L.L., and Keulegan, G.H., "Similitude Conditions in Free Surface Vortex Formations," Journal of Hydraulics Division, ASCE, Vol. 100, pp. 1565-1581, November 1974.

6. Reddy, Y.R., and Pickford, J., "Vortex Suppression in Stilling Pond Overflow," Journal of Hydraulics Division, ASCE, pp. 1685-1697, November 1974.

7. Durgin, W.W., and Hecker, G.E., "The Modeling of Vortices at Intake Structures," Joint Symposium on Design and Operation of Fluid Machinery, IAHR/ASME/ASCE, Colorado State University, June 1978.

8. Padmanabhan, M., and Vigander, S., "Pressure Drop Due to Flow through Fine Mesh Screens," Journal of Hydraulics Division, ASCE, August 1978.

ACKNOWLEDGEMENTS

This study involved many members of the ARL staff, and it is only possible to acknowledge their efforts collectively. A few individuals, however, have had a major influence on the study, and the author would like to cite these separately.

Professor George E. Hecker, Director, ARL, initiated this study and his guidance throughout the study is appreciated.

The fine work of construction and testing performed by Mr. Garreth Cooke, Engineering Associate, is acknowledged. Thanks are also due to Mr. Mark Majcher, graduate student, for his help during the last stages of testing and to Miss Nancy Vacca for typing the manuscript of this report.

M. Padmanabhan

TABLE 1

Operating Cases Tested

Operating Case No.	Flow/Pipe gpm	Range of Water Surface Elevation	Remarks
1a	9500	602'10" - 606'0"	Runout condition of one ECCS train upon complete failure of other. Left pipe operational.
1b	9500	602'10" - 606'0"	Runout condition of one ECCS train upon complete failure of other. Right pipe operational.
2	7700	606'0" - 612'0" (Minimum water level assumed at EL 602'10" for preliminary tests)	Runout condition of ECCS pumps with both trains operating.
3a	1 x 9500 1 x 3600	606'0" - 612'0"	Runout condition of one ECCS train (left); containment spray pump from other train at runout flow (right).
3b	1 x 3600 1 x 9500	606'0" - 612'0"	Runout condition of one ECCS train (right); containment spray pump from other train at runout flow (left).

TABLE 2

Farfield Observation Patterns
Affecting Approach Flow Distribution

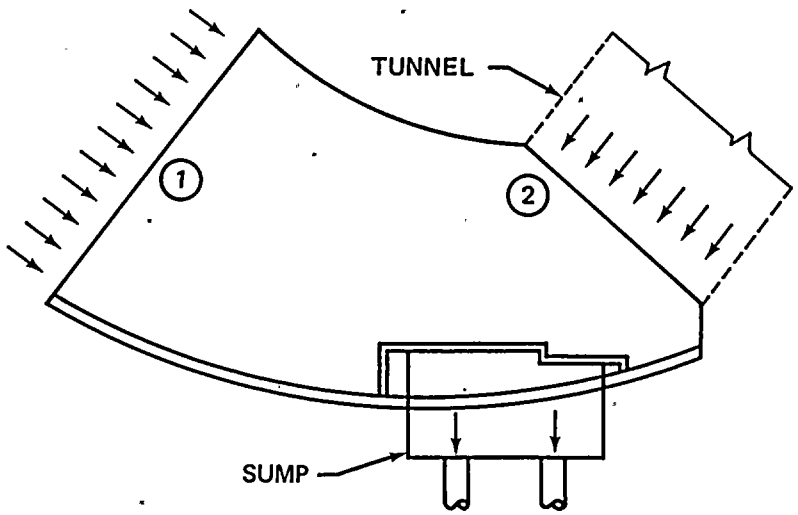

Obstruction Scheme No.	Percentage Open 1	2
1	100	100
2	0	100
3	100	0
4	50L	100
5	50R	100
6	50L	50L
7	50L	50R
8	50R	50L
9	50R	50R

TABLE 3

Preliminary Testing Series

Test No.	Operating Case No.	Water Level	Farfield Obstruction Scheme No.	Remarks
1	2	602'10"	1	
2	2	602'10"	2	
etc.	etc.	602'10"	etc.	Select 3 critical farfield obstructions CR1, CR2, CR3
9	2	602'10"	9	
10	1b	602'10"	CR1	
11	1b	602'10"	CR2	
12	1b	602'10"	CR3	
13	1b	612'0"	CR1	
14	1b	612'0"	CR2	
15	1b	612'0"	CR3	
16	1a	602'10"	CR1	
17	1a	602'10"	CR2	
18	1a	602'10"	CR3	
19	3a	602'10"	CR1	
20	3a	602'10"	CR2	
21	3a	602'10"	CR3	
22	3b	602'10"	CR1	
23	3b	602'10"	CR2	
24	3b	602'10"	CR3	
25	3b	612'0"	CR1	
26	3b	612'0"	CR2	
27	3b	612'0"	CR3	
28	2	612'0"	CR1	
29	2	612'0"	CR2	Select 3 critical combinations from tests 10 thru 30
30	2	612'0"	CR3	

TABLE 4

Effect of Grating Blockage on Vortexing and Swirl (Phase 2 Tests)

Test No.	Operating Case No.	50% Grating Blockage Scheme No.	F_r	Corresponding W.S. EL	Vortex Type	Indicated Swirl Angle deg.	Remarks
1	1a	1	1.58	602'10"	1, 2	2.6	Unstable Unsteady dimples
2	1a	2	1.58	602'10"	2, 3	3.1	Incoherent dye core
3	1a	3	1.58	602'10"	2, 3	3.2	Incoherent dye core
4	1a	4	1.58	602'10"	2, 3	1.4	Incoherent dye core
5	1a	5	1.58	602'10"	2, 3	3.3	Occasionally strong dye core
6	1a	6	1.58	602'10"	1, 2	2.2	Strong dimples
7	1a	7	1.58	602'10"	1	2.6	Practically no activity
8	2	1	1.58	602'10"	1, 2	1.8	Surface dimples
9	2	2	1.58	602'10"	2, 3	1.4	Weak dye core
10	2	3	1.58	602'10"	2, 4	1.3	Pulls trash to 6 inches
11	2	4	1.58	602'10"	2, 3	1.6	Occasional dye core
12	2	5	1.58	602'10"	2, 4	2.6	Pulls trash to 6 inches
13	2	6	1.58	602'10"	----	0.8	High turbulence weir flow over curb
14	2	7	1.58	602'10"	1	1.7	Mild surface swirls
15	2	3	1.0	602'10"	1, 2	1.4	Surface dimples
16	2	5	1.0	602'10"	1, 2	2.1	Unstable dimples

NOTE: Above observations were done before modifications to sump. Only selected runs showing severities included in this table.

TABLE 5

Effect of Perforated Plate Blockage on Vortexing and Swirl (Phase 2 Tests)

Test No.	Operating Case No.	50% Perforated Plate Blockage Scheme No.	50% Grating Blockage Scheme No.	Corresponding W.S. EL	Indicated Swirl Angle deg.	Remarks
1	1a	1	3	602'10"	1.1	Corner swirls observed
2	1a	2	3	602'10"	6.5	High swirl in suction pipe
3	1a	3	3	602'10"	1.7	Visible swirl at corners
4	1a	4	3	602'10"	1.1	Submerged air core due to swirl at corners
5	1a	5	3	602'10"	1.1	Visible swirl at corners
6	1a	6	3	602'10"	5.1	Intense swirl at corners
7	1a	2	2	602'10"	7.8	High swirl in suction pipe
8	1a	6	2	602'10"	5.6	High swirl in suction pipe
9	2	3	4	602'10"	11.4	Air bubbles come out of solution at certain locations
10	2	2	4	602'10"	18.1	Air bubbles come out of solution at certain locations

NOTE: Only selected runs showing severities included in this table.

TABLE 6

High Temperature-High Flow Tests on Original Sump

Test No.	Corresponding Prototype Discharge, gpm	Froude Number Ratio F_r	Water Temperature °F	Model Reynolds No. R x 10^{-5}	Indicated Swirl Angle deg.	Vortex Types Observed	Remarks
1	2 x 7700	0.8	59	2.58	3.7	1, 2	Only weak dimples
2	2 x 7700	1.0	60	3.23	3.7	1, 2	Only weak dimples
3	2 x 7700	1.2	57	3.58	3.9	1, 2	Only weak dimples
4	2 x 7700	1.4	59	4.37	4.3	2, 3, 4	Incoherent dye cores and at times trash pulling
5	2 x 7700	1.6	60	5.10	3.9	2, 3, 4	Occasional trash pulling
6	2 x 7700	1.8	62	5.90	4.1	2, 3, 4	Occasional trash pulling
7	2 x 7700	0.8	94	4.04	2.0	1, 2	Weak dimples
8	2 x 7700	1.0	94	5.19	2.1	1, 2	Weak dimples
9	2 x 7700	1.2	95	6.07	2.3	1, 2, 3	Occasional weak dye core
10	2 x 7700	1.4	95	7.08	2.3	2, 3, 4	At times pulls trash to 6 inches
11	2 x 7700	1.6	94	8.29	1.6	2, 3, 4	Occasional trash pulling
12	2 x 7700	0.8	133	5.72	1.4	1, 2	Weak dimples
13	2 x 7700	1.0	134	7.05	1.6	1, 2	Weak dimples
14	2 x 7700	1.2	133	8.61	1.5	1, 2, 3	Occasional weak dye core
15	2 x 7700	1.4	133	10.03	1.5	2, 3, 4	Occasional trash pulling

TABLE 6
(Continued)

Test No.	Corresponding Prototype Discharge, gpm	Froude Number Ratio F_r	Water Temperature °F	Model Reynolds No. R x 10^{-5}	Indicated Swirl Angle deg.	Vortex Types Observed	Remarks
16	2 x 7700	1.6	137	11.06	2.0	2, 3, 4	Occasional trash pulling
17	2 x 7700	0.8	160	6.94	1.9	1, 2	Weak dimples
18	2 x 7700	1.0	160	8.92	1.4	1, 2	Weak dimples
19	2 x 7700	1.2	170	11.55	1.4	1, 2, 3	Occasional dye core
20	2 x 7700	1.4	168	13.14	1.1	2, 3, 4	Occasional trash pulling
21	2 x 7700	1.6	167	15.00	1.5	2, 3, 4	Occasional trash pulling

NOTE: The test conditions are a) operating case 2
b) W.S. EL 602'10"
c) grating blocked 50% as per scheme 3
d) perforated plate not blocked

TABLE 7

Effect of Grating Blockage on Vortexing and Swirl
(Phase 3 Tests) for Modified Sump

Test No.	Operating Case No.	50% Grating Blockage Scheme No.	F_r	Corresponding W.S. EL	Vortex Type	Indicated Swirl Angle deg.	Remarks
1	1a	No blockage	1.58	602'10"	1, 2	4.8	Intermittent unstable dimples fed by eddies
2	1a	1	1.58	602'10"	1, 2	3.5	Intermittent unstable dimples fed by eddies
3	1a	2	1.58	602'10"	2, 3	3.9	Occasional weak dye core
4	1a	3	1.58	602'10"	1, 2	3.9	Strong dimples
5	1a	4	1.58	602'10"	2, 3	1.8	Weak dye cores at times
6	1a	5	1.58	602'10"	2, 3	3.3	Occasional strong dye core
7	1a	6	1.58	602'10"	Unidentifiable	4.1	Weir flow over curb High turbulence
8	1a	7	1.58	602'10"	1	4.2	Little surface activity
9	2	5	1.58	606'0"	1, 2, 3	3.3	Wandering vortices outside sump. Occasional dye core, but core did not penetrate screen.
10	2	5	1.0	606'0"	1, 2	---	Eddies shed by obstructing structures
11	1a	5	1.0	602'10"	1, 2	---	Weak dimples
12	3a	5	1.58	612'0"	1	---	Only eddies
13	3a	5	1.58	608'3"	1, 2	---	Surface dimples
14	2	5	1.58	612'0"	1	---	Only eddies

TABLE 8

High Temperature-High Flow Tests on Modified Sump

Test No.	Operating Case No.	F_r	Water Temperature °F	Model Reynolds No. R x 10^{-5}	Vortex Types Observed	Remarks
1	1a	1.0	66	4.33	1, 2	Only weak dimples
2	1a	1.58	66	6.84	2, 3	Occasional dye cores, extending to about 6 inches deep
3	1a	1.8	66	7.79	2, 3	Occasional dye cores, extending to about 6 inches deep
4	1a	2.0	66	8.66	2, 3, 4	Rarely strong enough to pull trash
5	1a	1.0	96	6.22	1, 2	Weak dimples
6	1a	1.58	96	9.82	2, 3	Weak dye core type vortices, unstable
7	1a	1.8	96	11.19	2, 3	Weak dye core type vortices, unstable
8	1a	2.0	96	12.44	3, 4	At times trash pulling
9	1a	1.0	138	9.33	1, 2	Weak dimples
10	1a	1.58	138	14.74	2, 3	Weak dye core
11	1a	1.8	138	16.78	2, 3	Weak dye core
12	1a	2.0	138	18.66	3, 4	Occasionally trash pulling
13	1a	1.0	164	11.54	1, 2	Weak dimples
14	1a	1.58	164	18.24	2, 3	Weak dye core
15	1a	1.8	164	20.78	2, 3	Weak dye cores
16	1a	2.0	164	23.08	3, 4	Rare trash pulling

NOTE: Tests were done with grating blockage of scheme 5 at water surface elevation corresponding to 602'10".

TABLE 9

Evaluation of Inlet Loss Coefficients - Original Sump

Test No.	Water Temperature °F	Pipe No.	u fps	$u^2/2g$ ft	R x 10^{-5}	Grating/Screen Blockage Scheme No.	C_L	Remarks
1	59	1	5.60	0.486	2.58	3	0.23	Both pipes operating
2	60	1	7.01	0.762	3.23	3	0.26	Both pipes operating
3	57	1	8.25	1.056	3.57	3	0.27	Both pipes operating
4	59	1	9.64	1.442	4.37	3	0.26	Both pipes operating
5	60	1	11.01	1.883	5.08	3	0.27	Both pipes operating
6	62	1	12.61	2.470	5.90	3	0.25	Both pipes operating
7	64	1	8.63	1.157	4.17	3	0.21	One pipe operating
8	95	1	11.20	1.946	8.29	3	0.27	Both pipes operating
9	95	1	7.01	0.762	5.19	3	0.25	Both pipes operating
10	137	1	11.20	1.946	11.06	3	0.28	Both pipes operating
11	134	1	7.01	0.762	7.05	3	0.27	Both pipes operating
12	59	1	7.01	0.762	3.18	5	0.22	Both pipes operating
13	95	1	11.20	1.946	8.29	5	0.30	Both pipes operating
14	134	1	7.01	0.762	7.05	5	0.24	Both pipes operating
15	57	2	4.20	0.273	1.82	3	0.22	Both pipes operating
16	61	2	9.76	1.480	4.58	3	0.26	Both pipes operating
17	63	2	13.78	2.950	6.45	3	0.25	One pipe operating
18	59	2	11.15	1.932	4.83	None	0.20	Both pipes operating No blockage of gratings

NOTE: All observations were at minimum water level with 50% grating blockage (scheme 3).

TABLE 10

Evaluation of Inlet Loss Coefficients - Modified Sump

Test No.	Pipe No.	u fps	$u^2/2g$ ft	R x 10^{-5}	C_L	Remarks
1	1	5.17	0.415	2.67	0.26	One pipe operating
2	1	8.62	1.153	4.45	0.29	One pipe operating
3	1	13.79	2.954	7.12	0.26	One pipe operating
4	2	8.62	1.153	4.45	0.22	One pipe operating
5	1	5.59	0.485	2.88	0.21	Both pipes operating
6	1	11.18	1.941	5.77	0.25	Both pipes operating
7	2	4.19	0.272	2.16	0.22	Both pipes operating
8	2	6.99	0.757	3.61	0.22	Both pipes operating
9	2	9.79	1.485	5.05	0.22	Both pipes operating
10	2	12.58	2.455	6.49	0.28	Both pipes operating

NOTE: All observations were at minimum water level with 50% screen blockage (scheme 5).

TABLE 11

Original versus Modified Sump Design

Description	Sump Design	
	Original	Revised
Vortex type of highest severity with 50% screen blockage	Trash pulling (type 4)	Weak unstable dye core (type 3)
Maximum indicated swirl	7.8 degrees	4.2 degrees
Fine mesh screen	Horizontal perforated plate but no vertical fine screens	Vertical fine mesh screen behind grating
Air-venting at top covers	Not sufficient	Additional vent pipes or holes are to be provided
Inlet loss coefficient	0.26	0.24

PHOTOGRAPHS

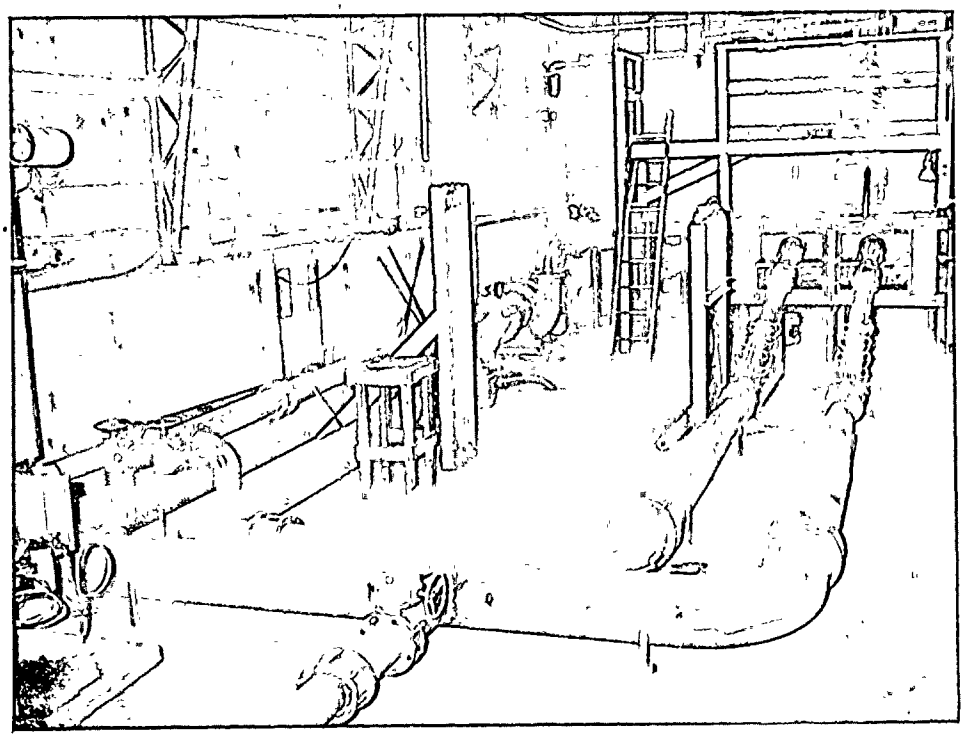

Photograph 1 Containment Recirculation Sump Model

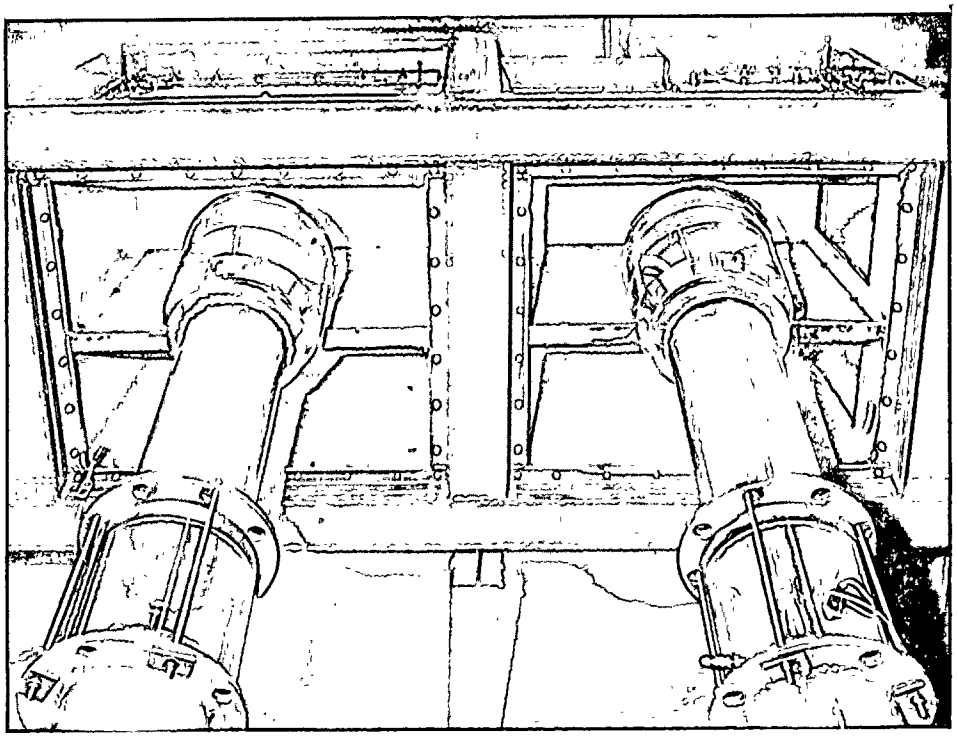

Photograph 2 Suction Pipe Layout

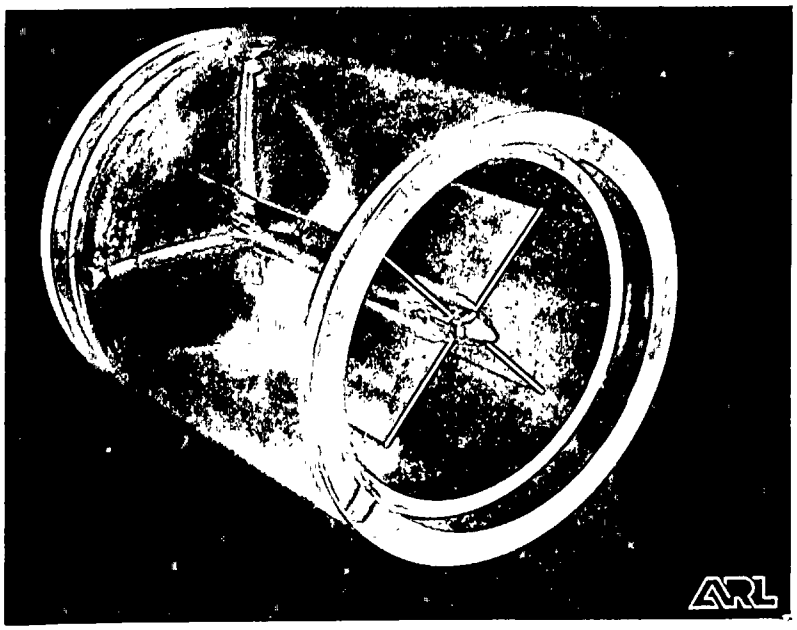

Photograph 3 Vortimeter for Swirl Measurements

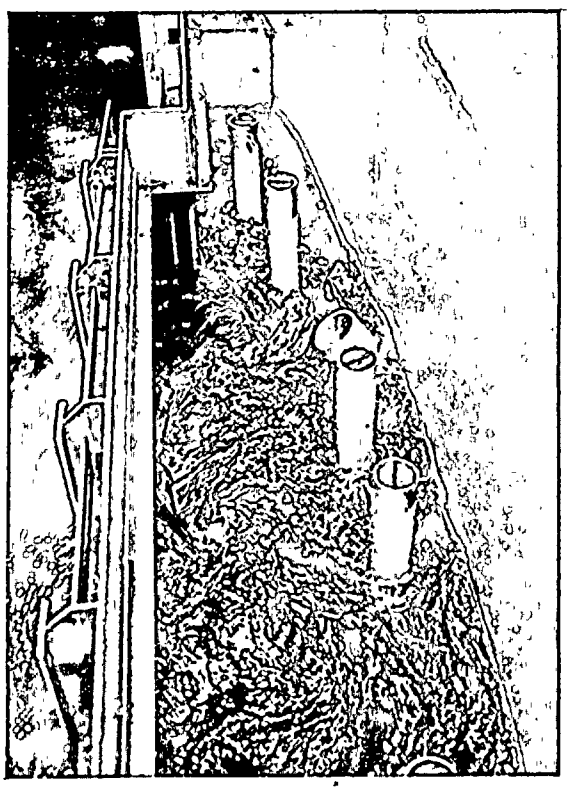

Photograph 4 Vortex Activity Inside Sump; Original Design; F_r = 1.58; Operating Case 2, Grating Blockage Scheme 3

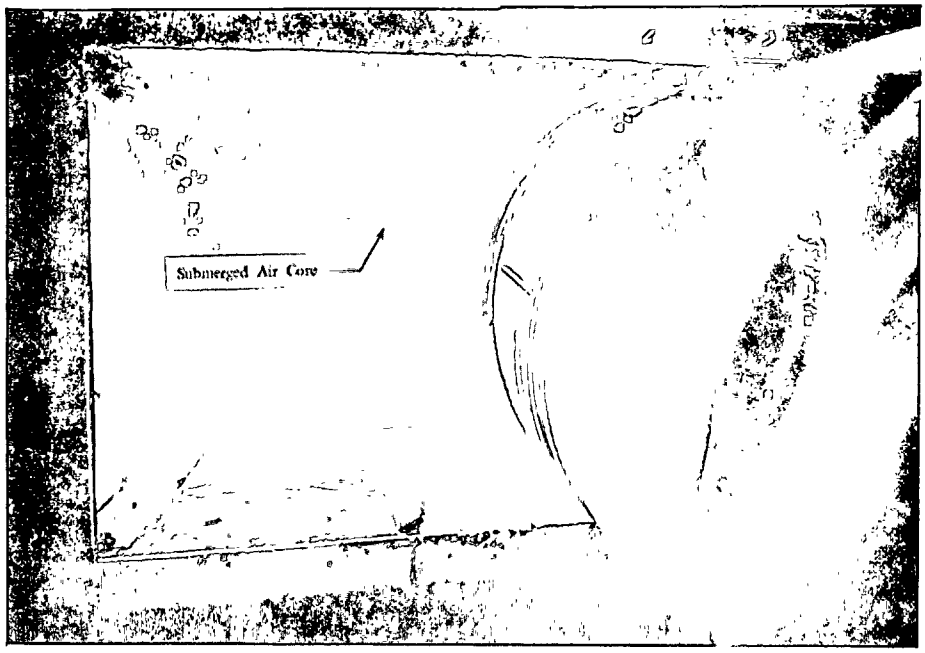

Photograph 5 Submerged Air-Core Observed During Perforated Plate Blockage Tests; F_r = 1.58; Operating Case 2, Blockage Scheme 4

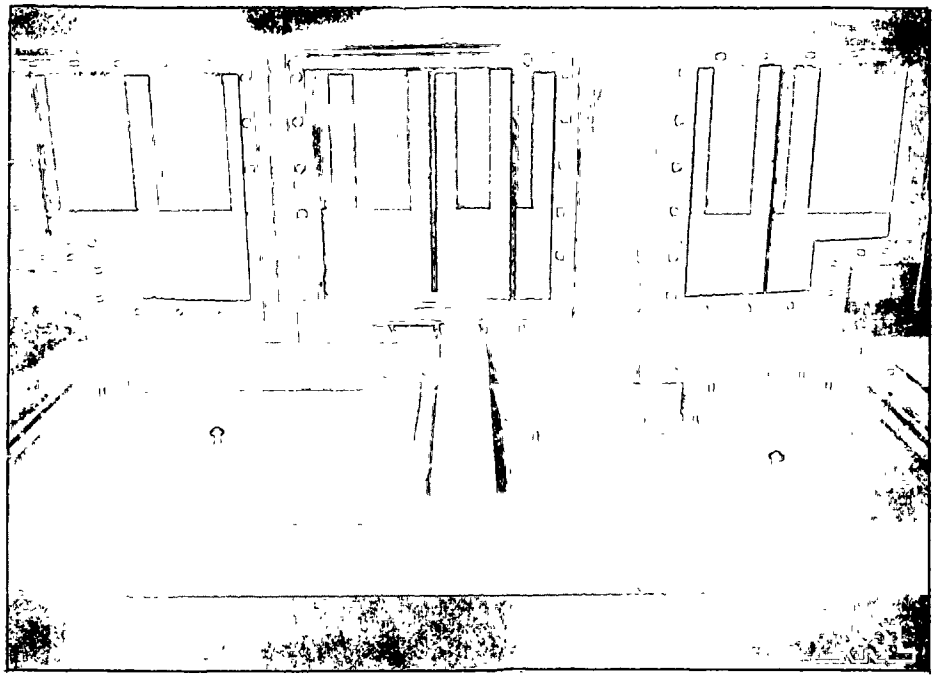

Photograph 6 Modified Sump

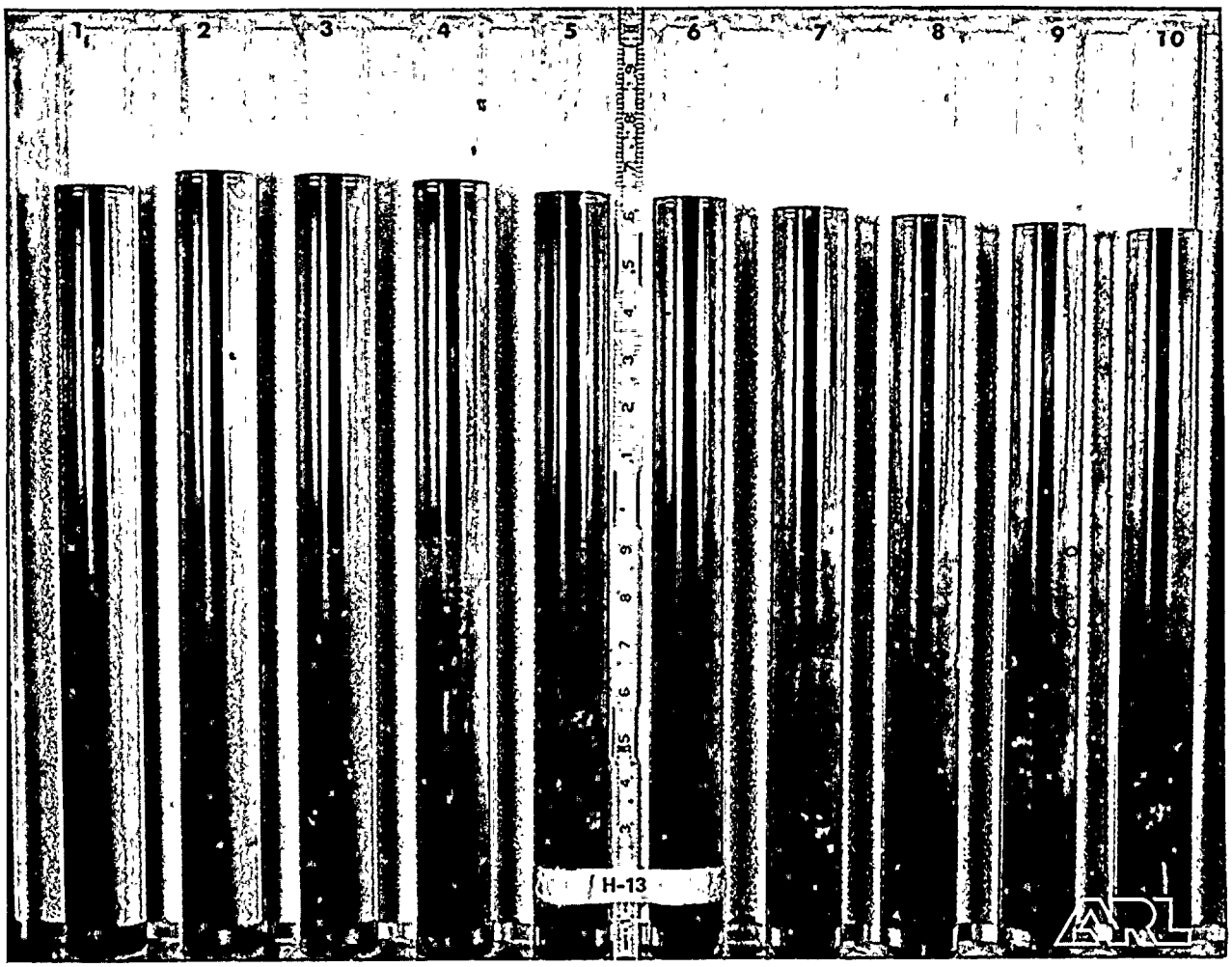

Photograph 7 Pressure Gradient in Pipe 1; Modified Sump; F_r = 1.00; Operating Case 2; Grating Blockage Scheme 3

FIGURES

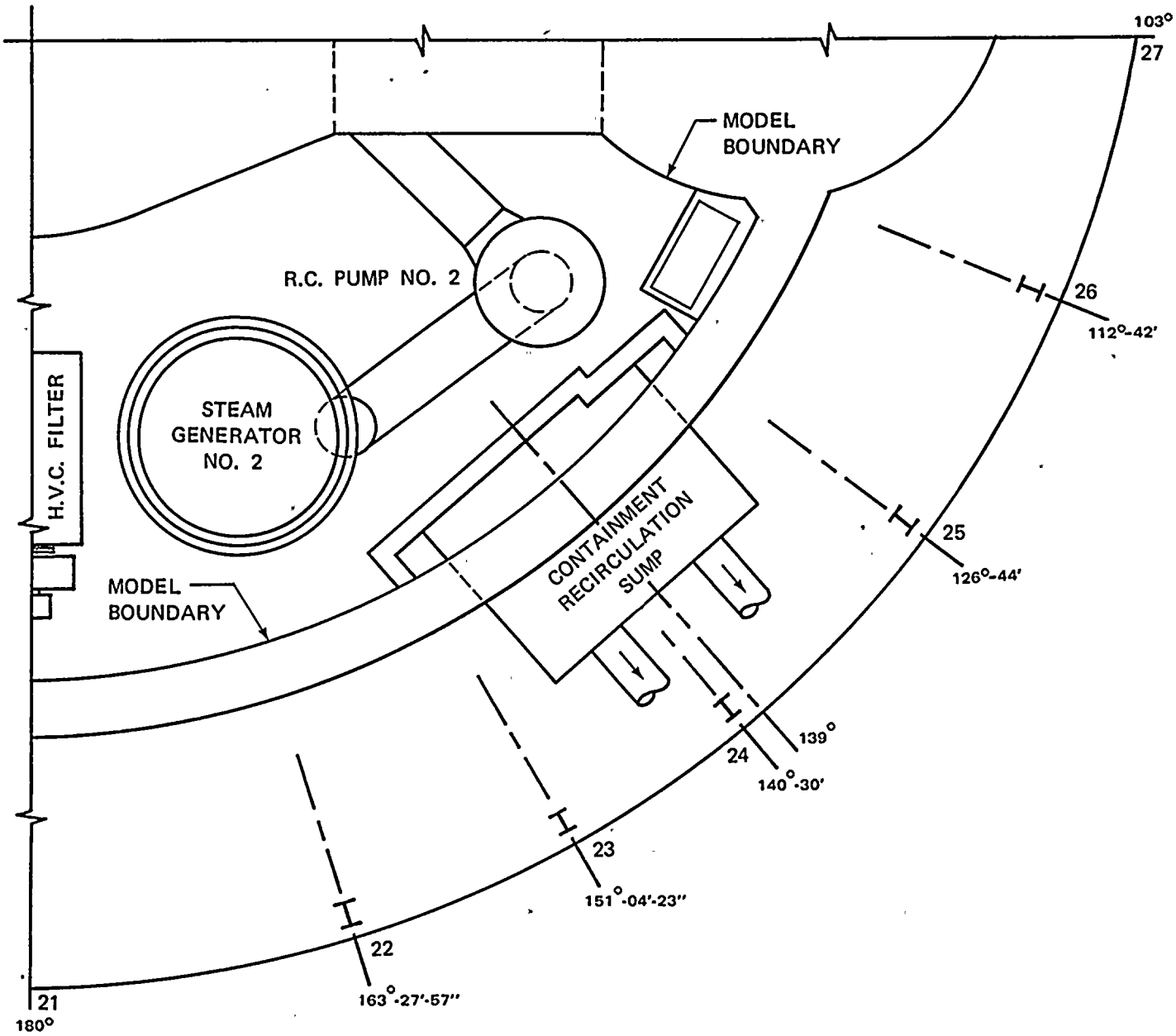

FIGURE 1 LOCATION OF SUMP WITHIN CONTAINMENT BUILDING

ARL

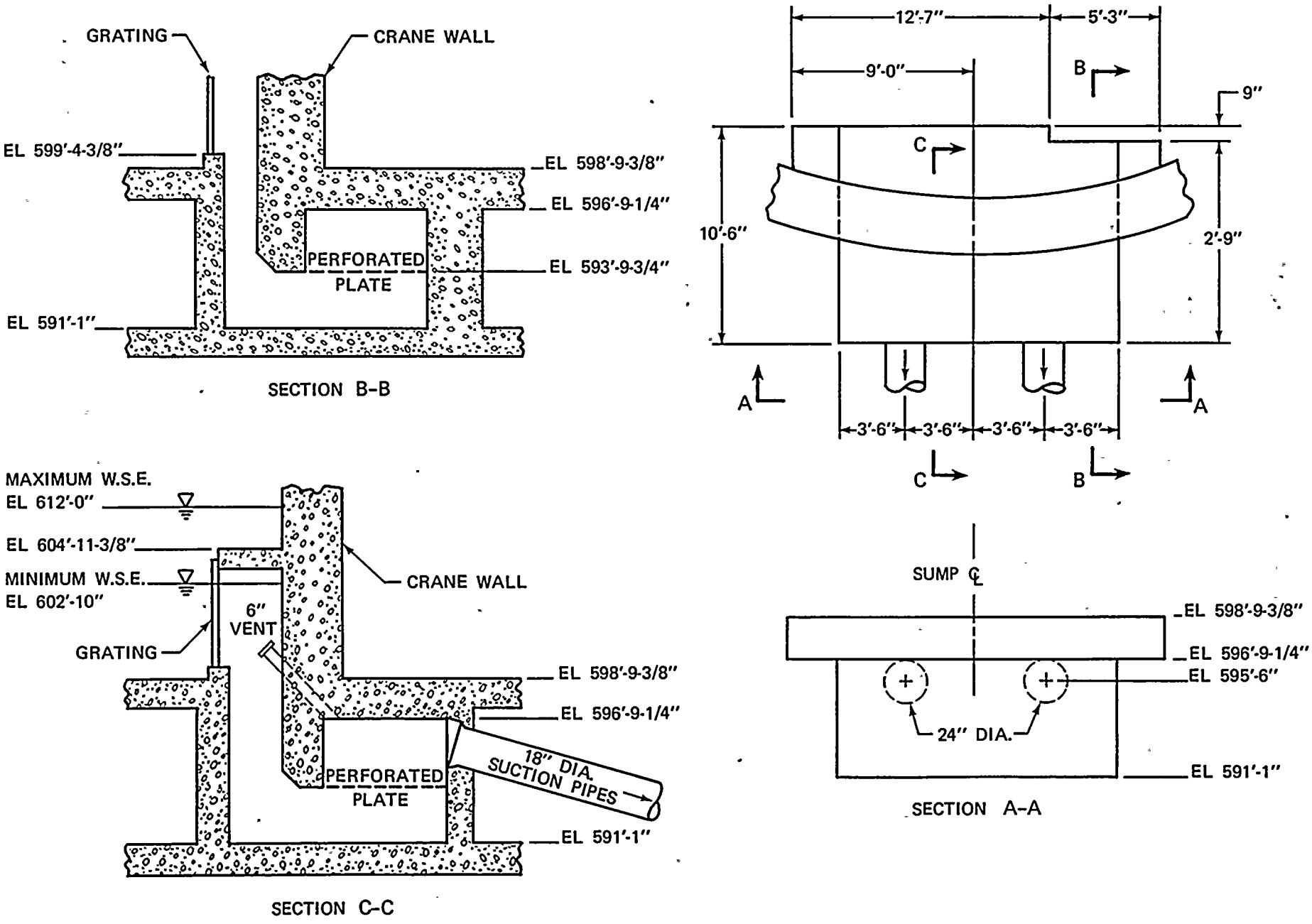

FIGURE 2 DETAILS OF ORIGINAL SUMP

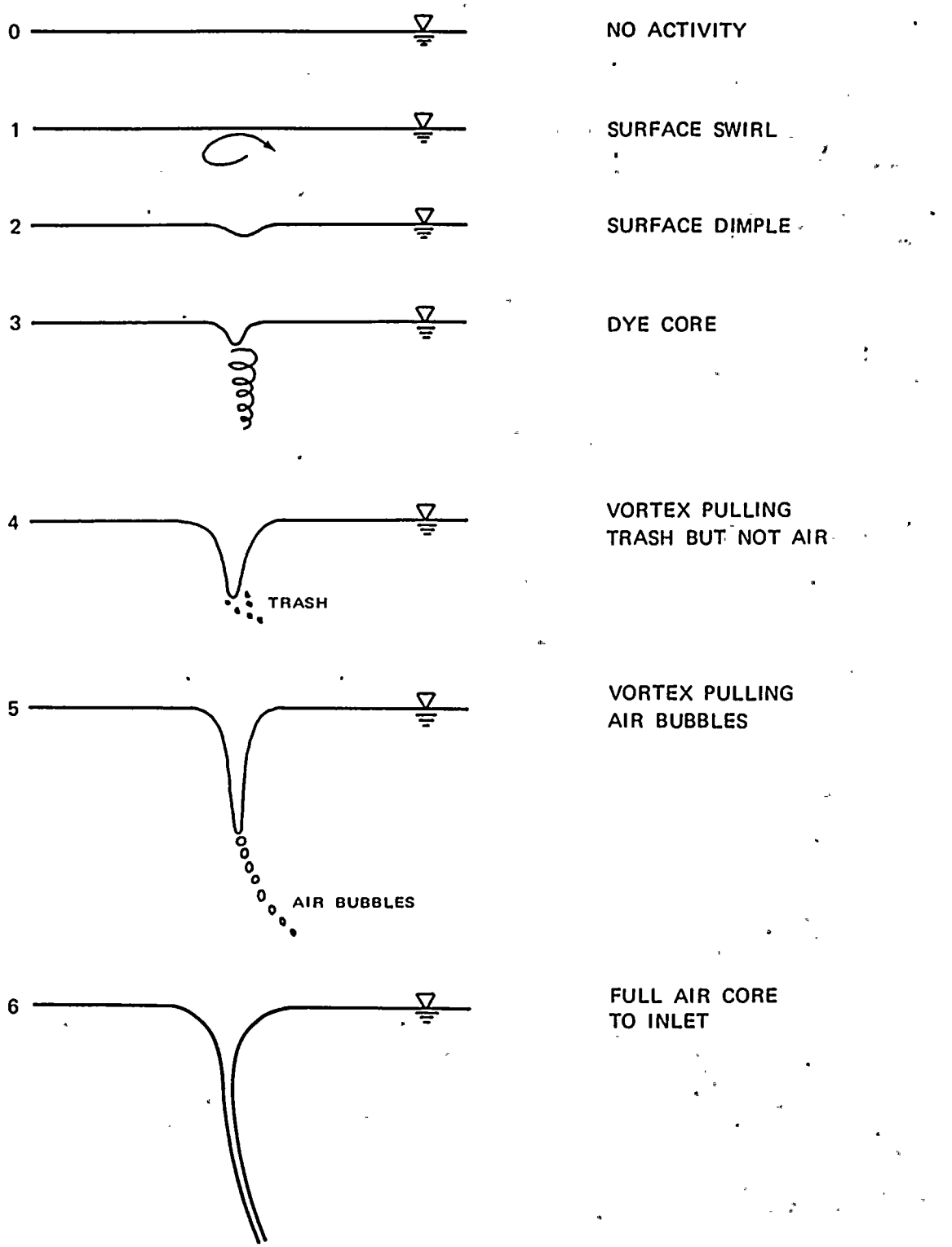

FIGURE 3 VORTEX STRENGTH SCALE FOR INTAKE STUDY

ARL

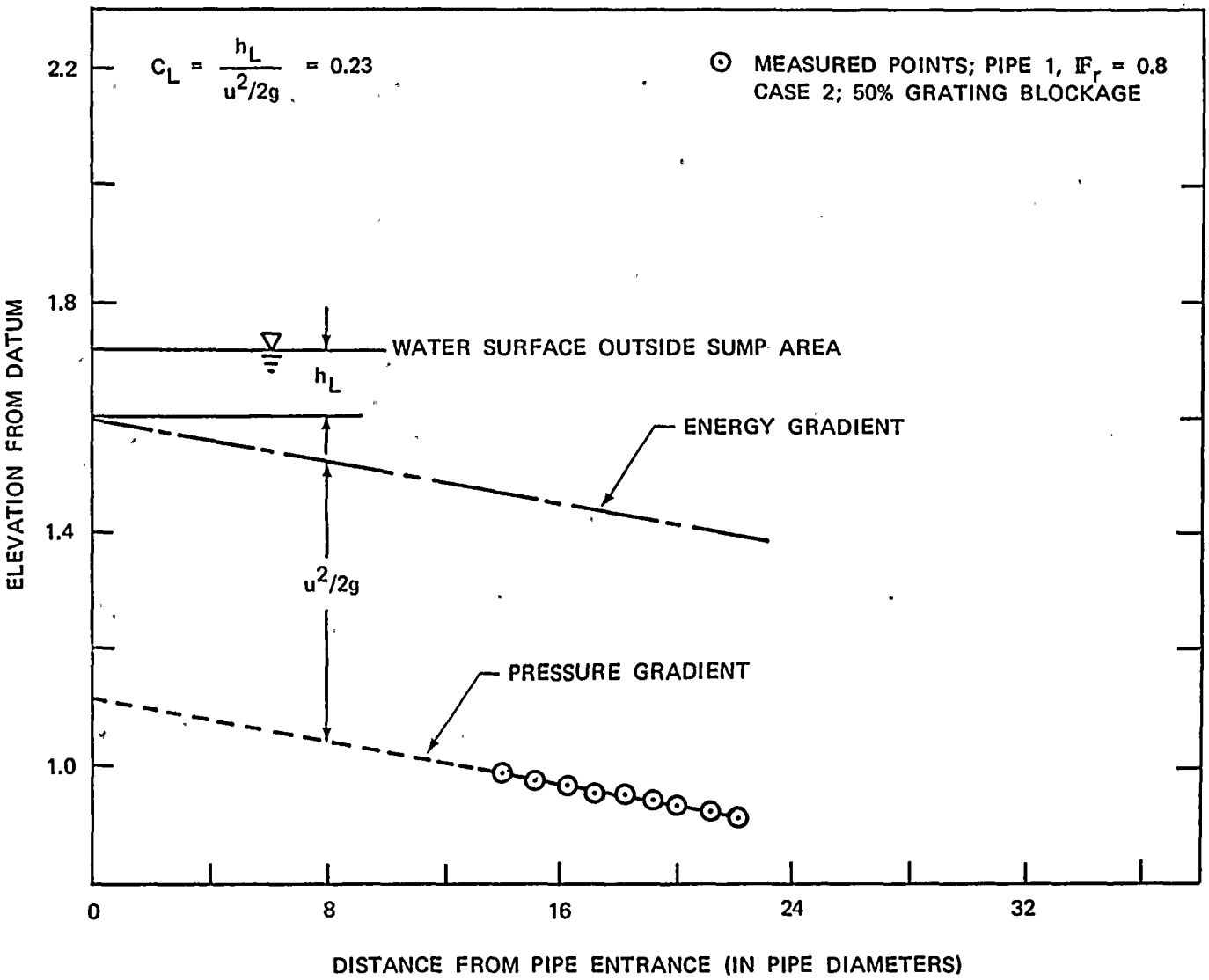

FIGURE 4 EVALUATION OF INLET LOSS COEFFICIENT, C_L

$$IF_r = \frac{IF_m}{IF_p}$$

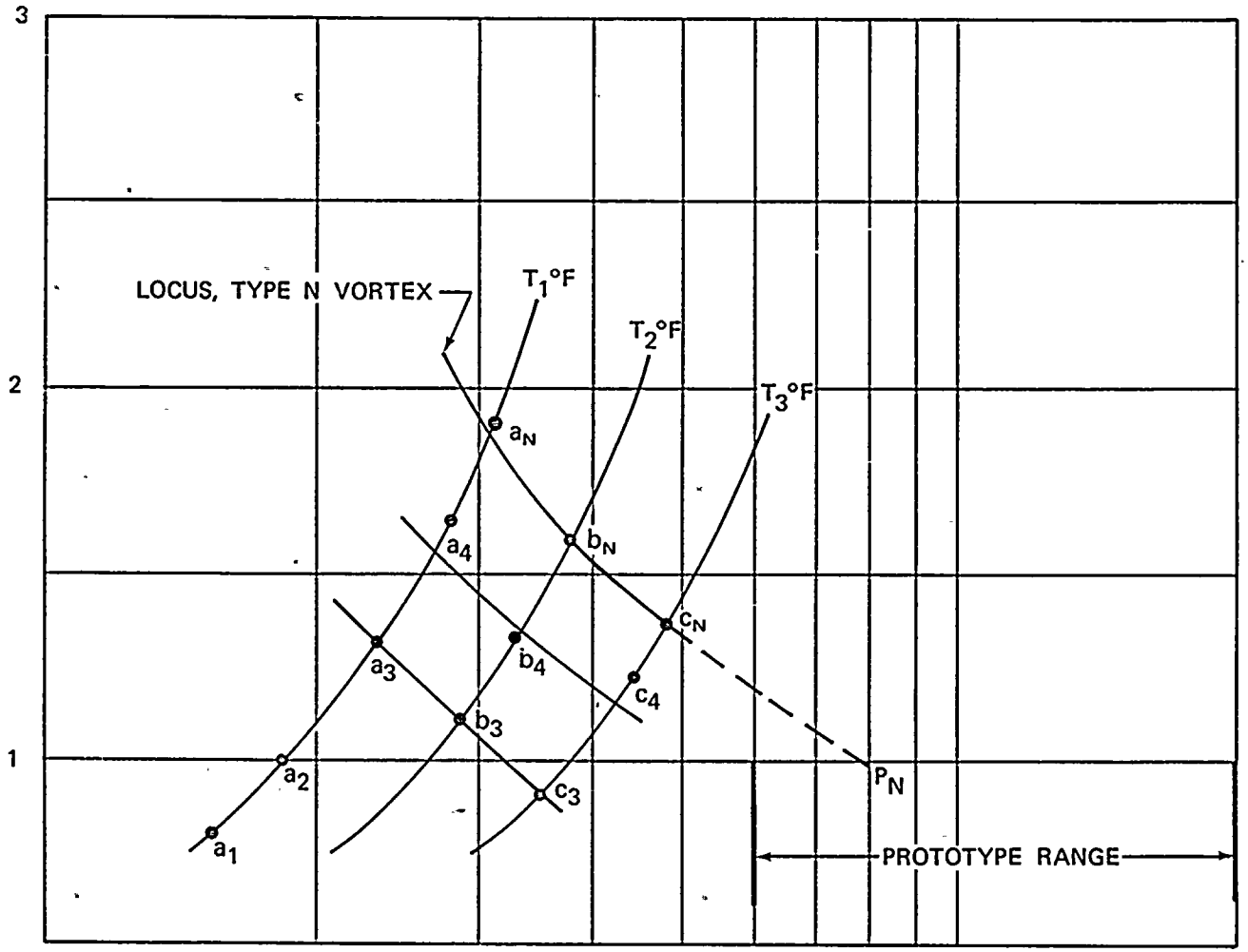

FIGURE 5 DEPENDENCE OF VORTEX SEVERITY ON FROUDE AND REYNOLDS NUMBERS

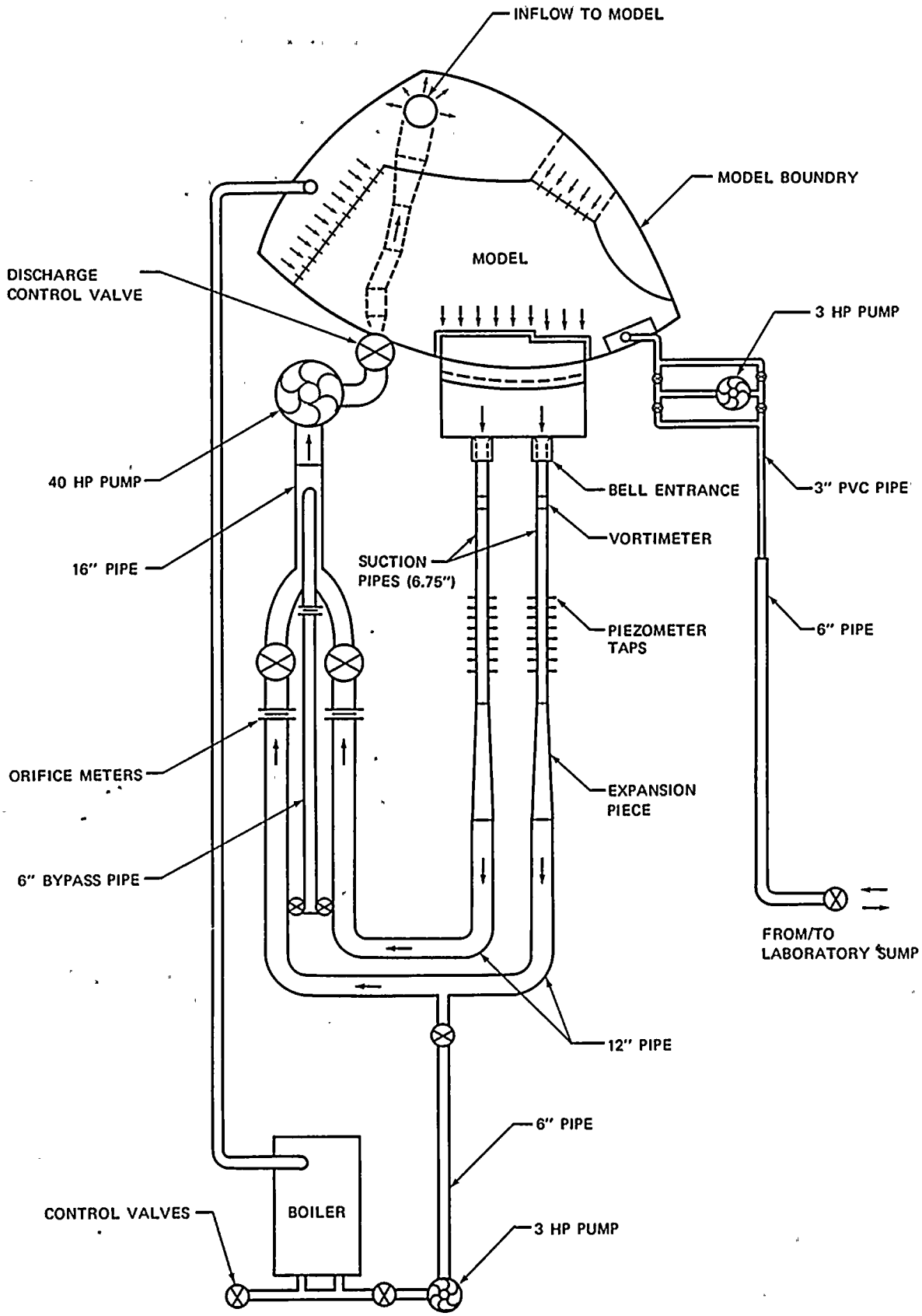

FIGURE 6 PIPE LAYOUT IN THE MODEL

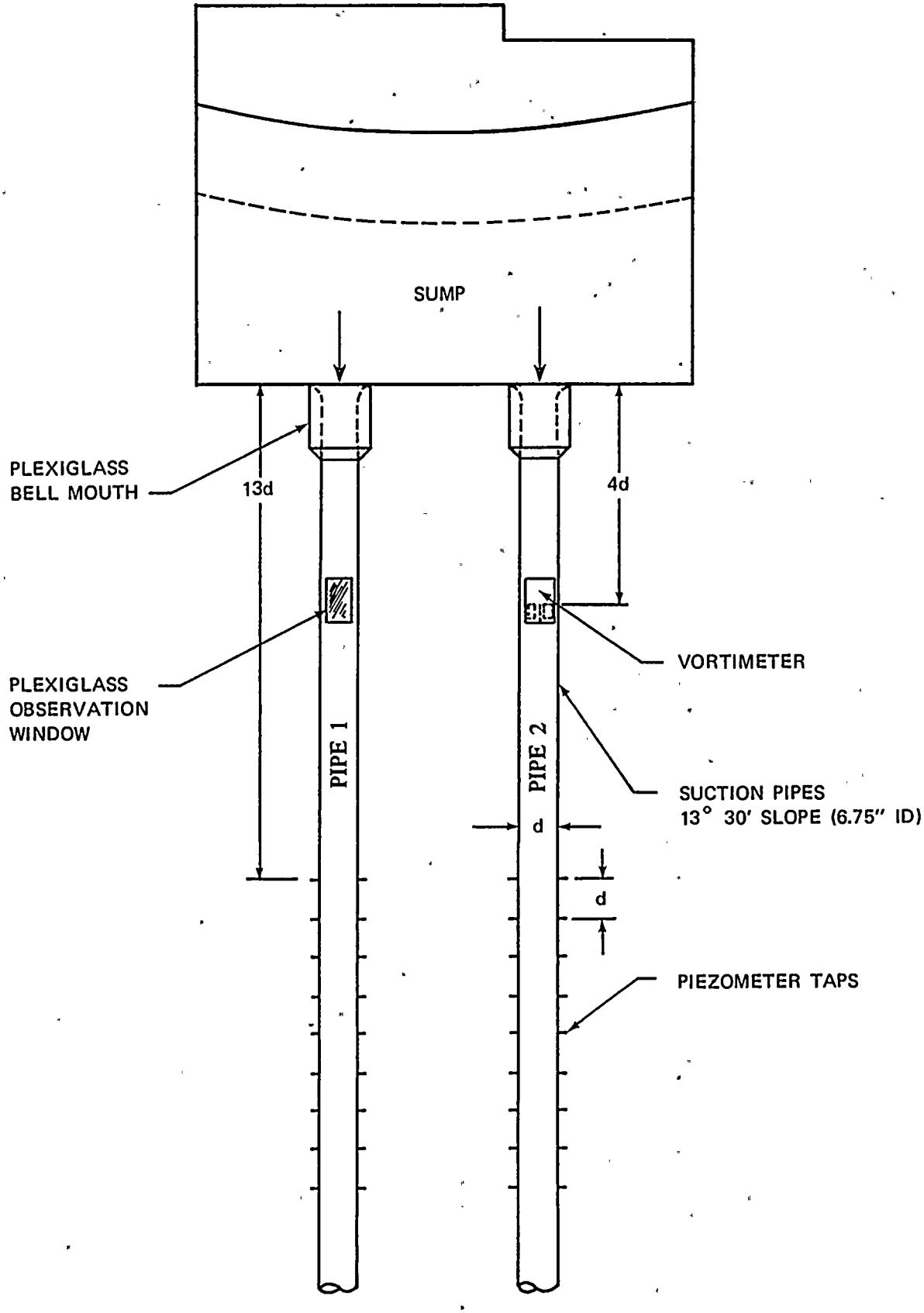

FIGURE 7 SUCTION PIPES IN MODEL

ARL

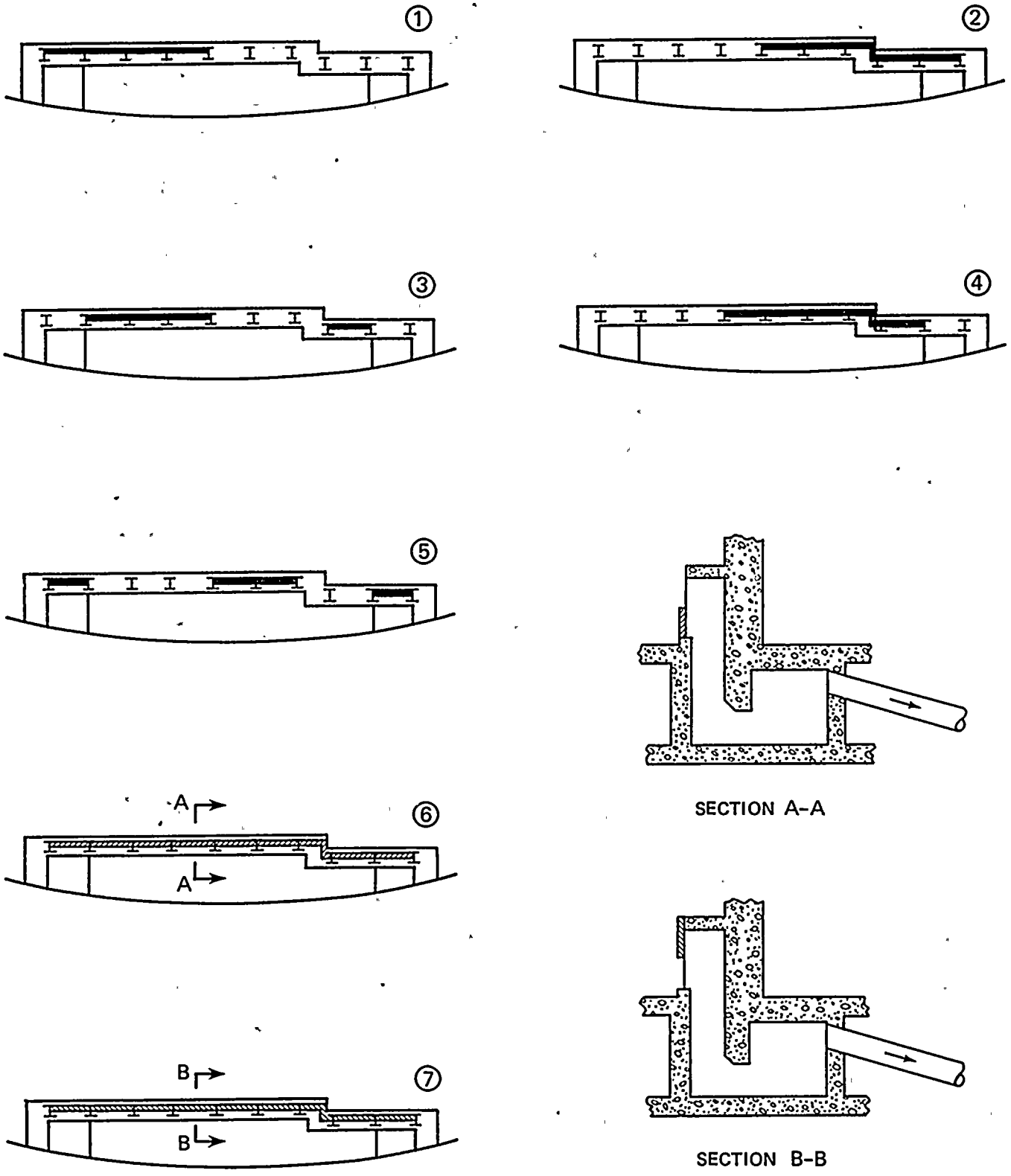

FIGURE 8 BLOCKAGE SCHEMES ON VERTICAL GRATING

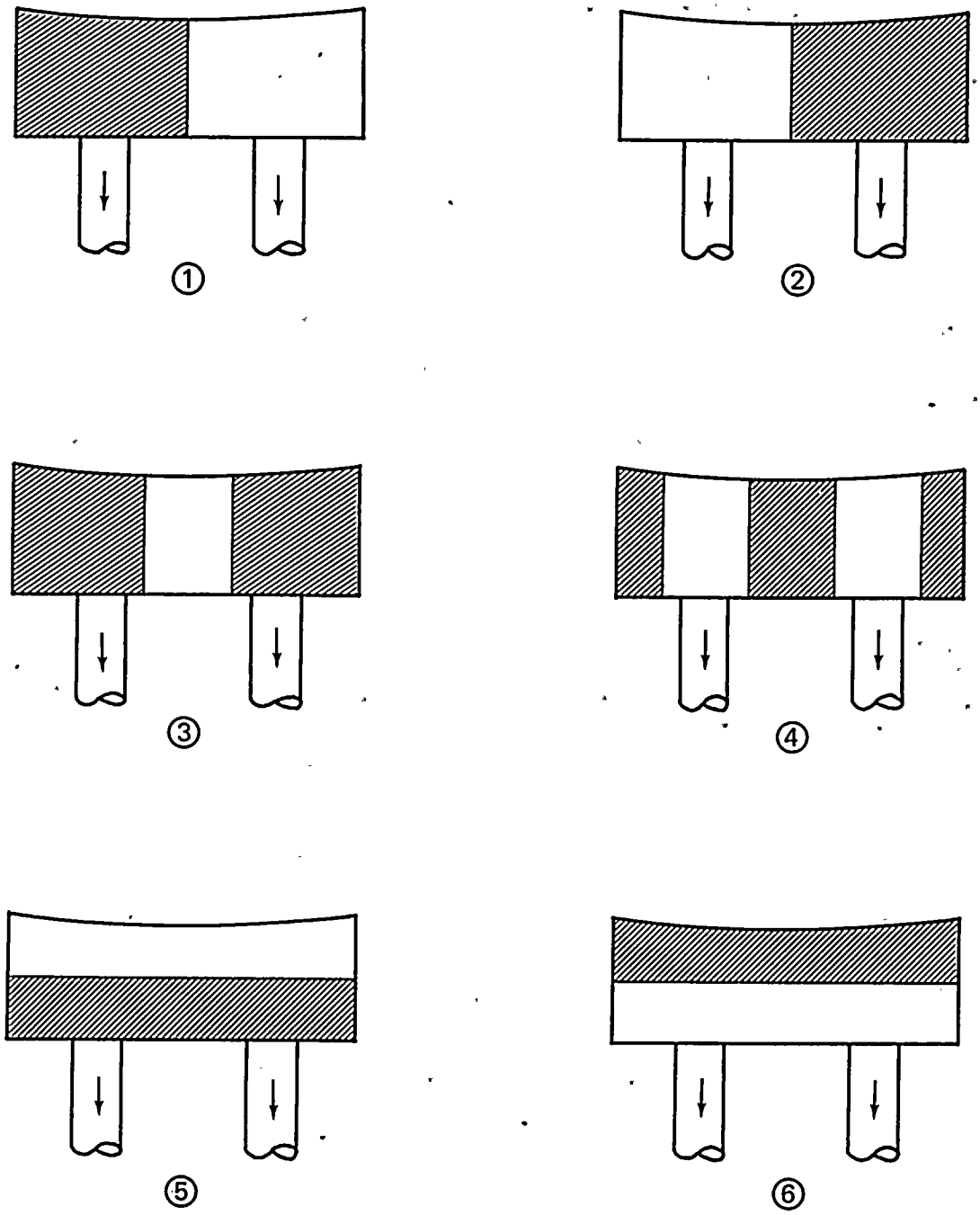

FIGURE 9 BLOCKAGE SCHEMES ON PERFORATED PLATE

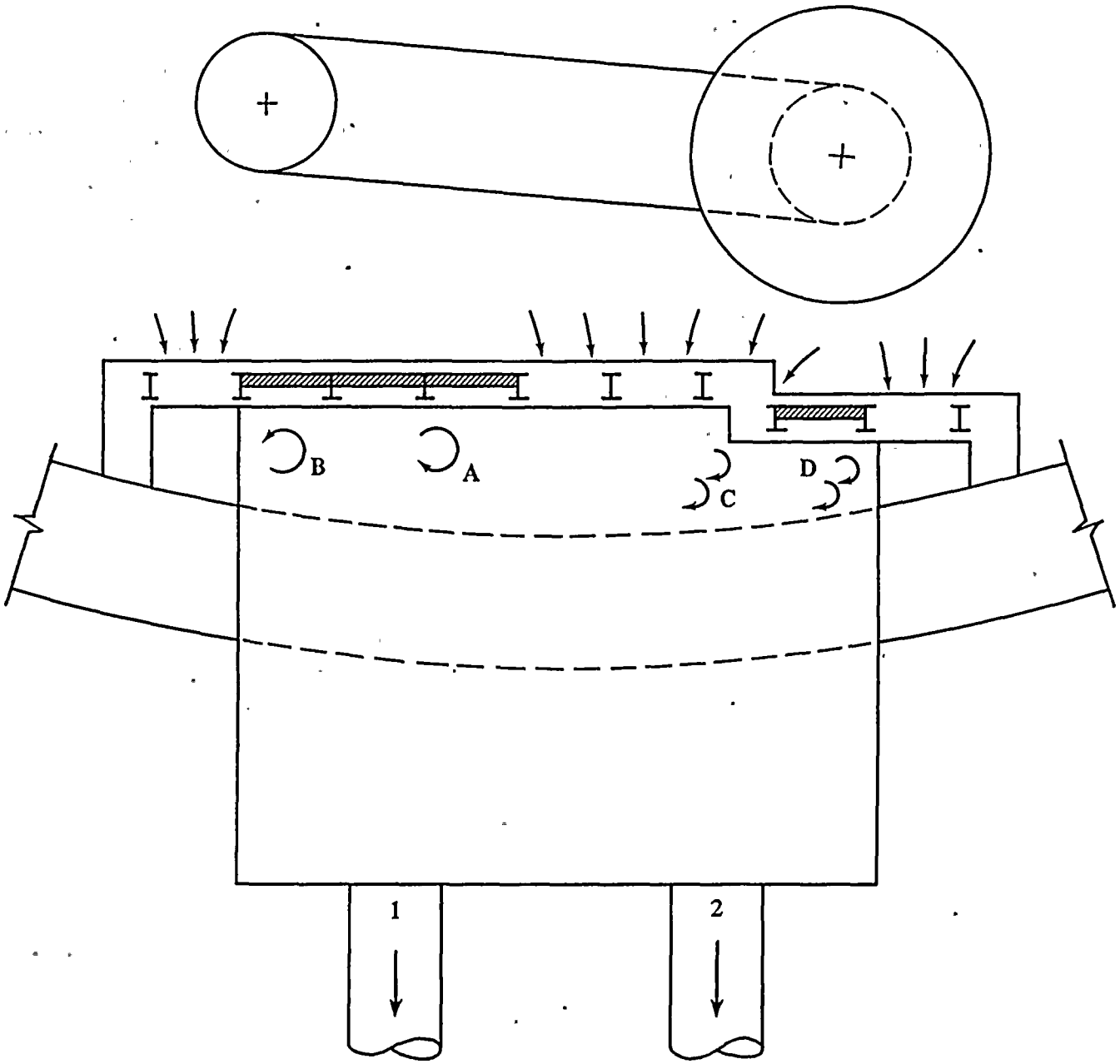

A & B	VORTICES OF TYPE 2-4, UNSTABLE AND INTERMITTENT
C & D	EDDIES SHED; OCCASIONAL DIMPLES

GRATING BLOCKAGE SCHEME 3; NO PERFORATED PLATE BLOCKAGE

FIGURE 10 VORTEXING INSIDE SUMP; CASE 2; W.S. EL 602'-10"
OBSERVED DURING HIGH TEMPERATURE-HIGH VELOCITY TESTS

ARL

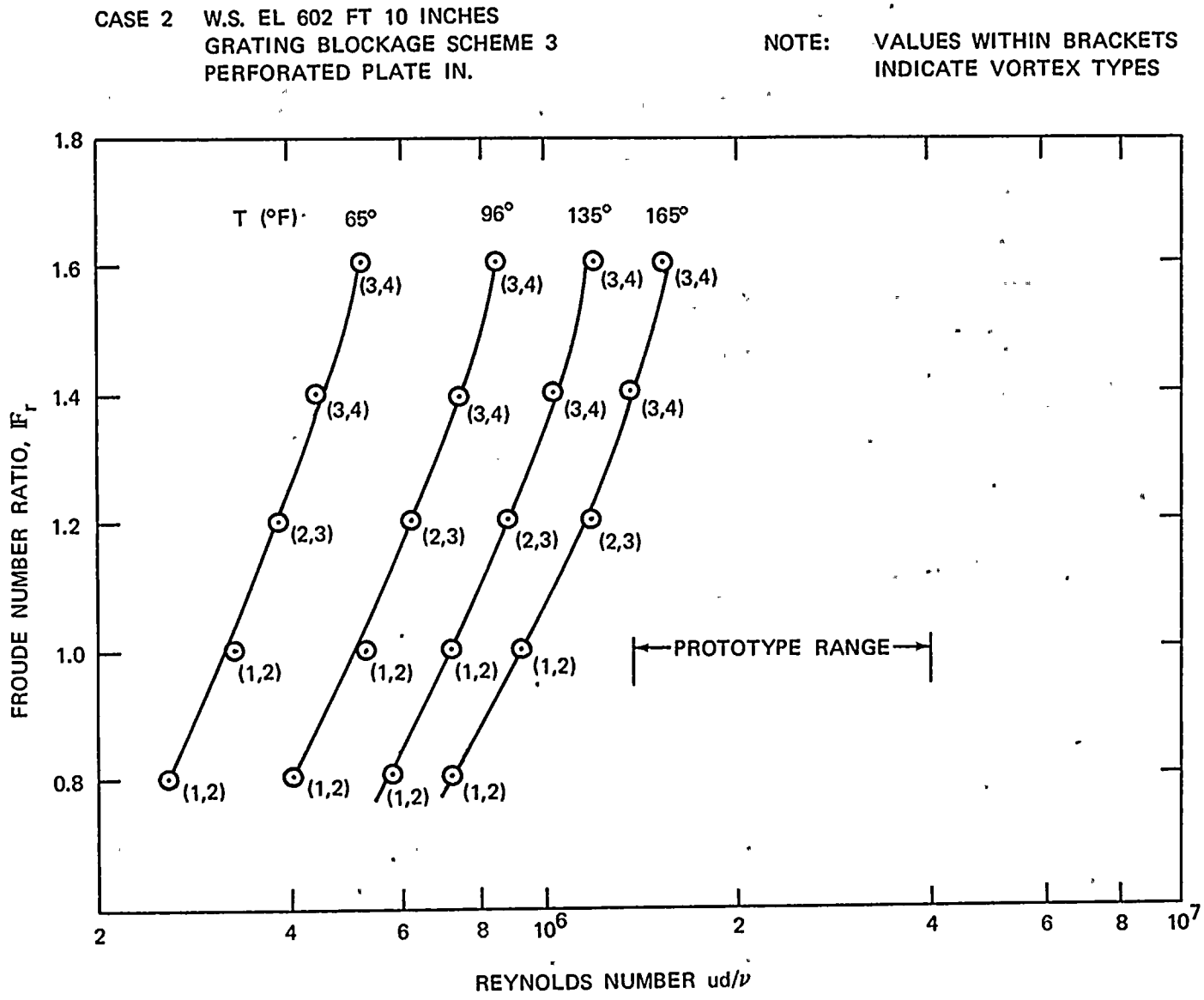

FIGURE 11 VORTEX SEVERITIES OBSERVED DURING HIGH-TEMPERATURE-HIGH VELOCITY TESTS

CASE 2: W.S. EL 602 FT 10 INCHES
GRATING BLOCKAGE SCHEME 3
PERFORATED PLATE IN.

NOTE: VALUES WITHIN BRACKETS INDICATE VORTIMETER REVOLUTIONS/2 MINUTES

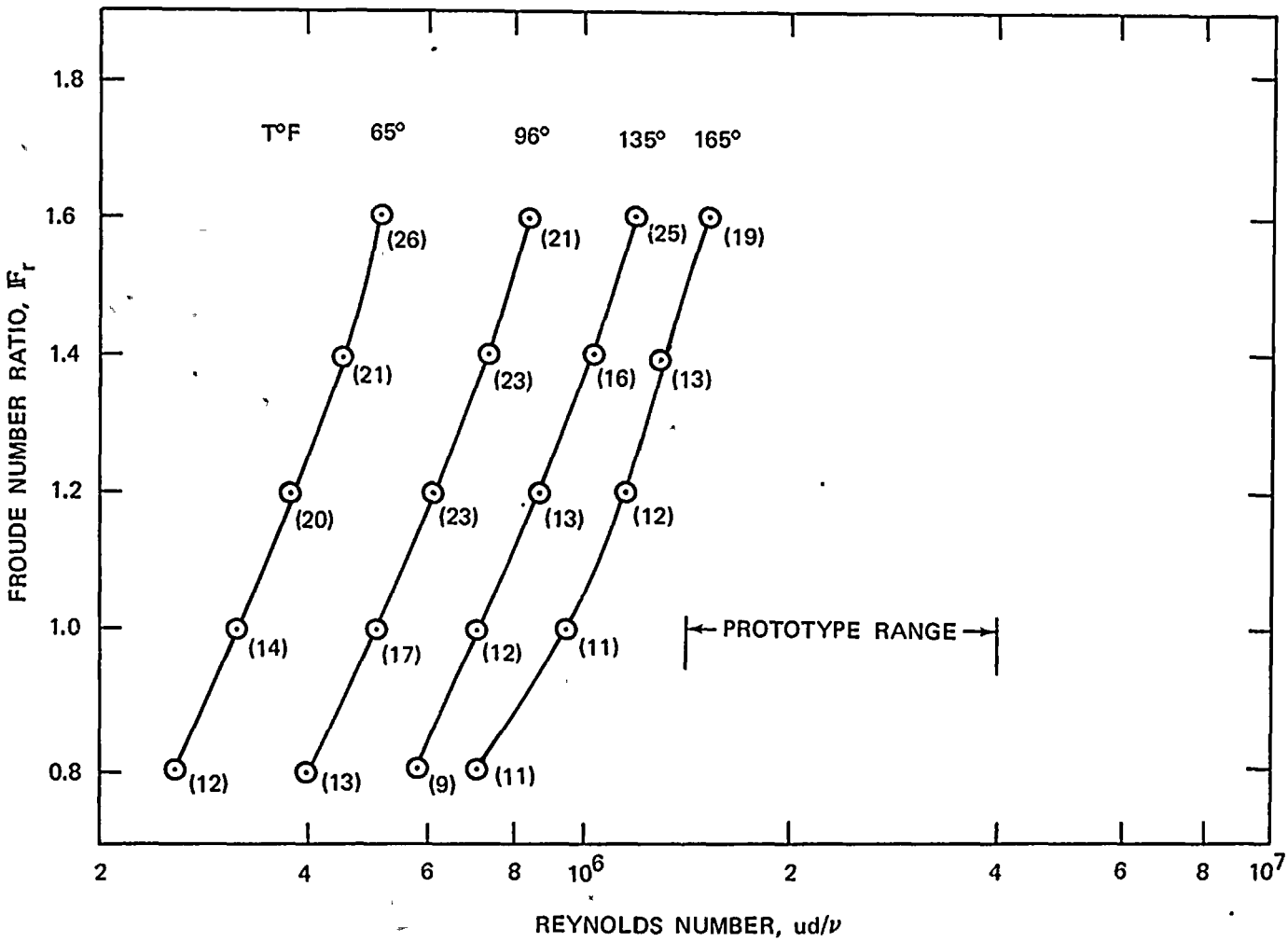

FIGURE 12 SWIRL DURING HIGH TEMPERATURE-HIGH VELOCITY TESTS

ARL

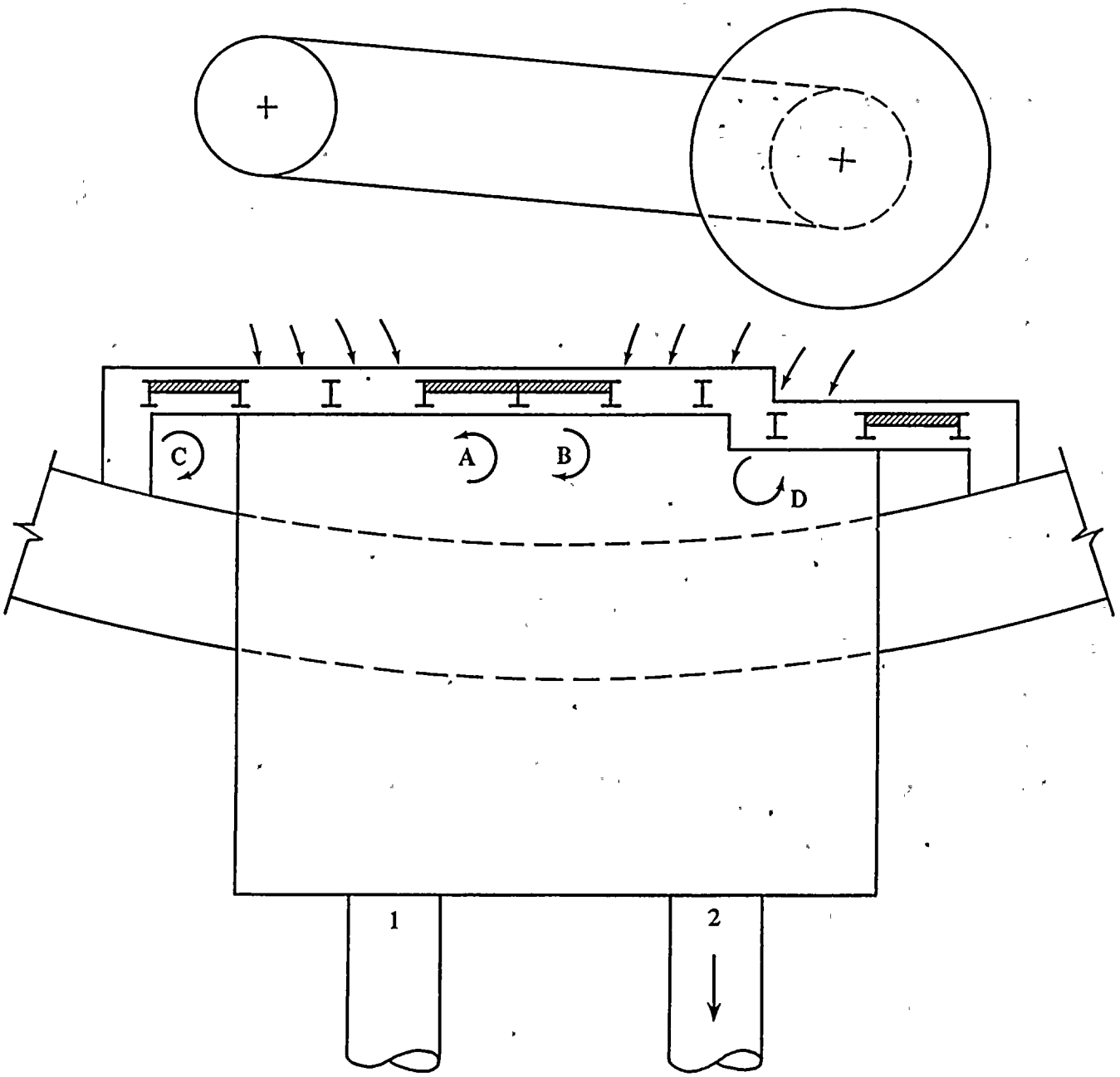

A & B	TYPE 1 TO 2 FOR F_r = 1.0 TYPE 2 TO 3 FOR F_r = 1.58 UNSTABLE AND INTERMITTENT
C	TYPE 1 TO 2 FOR F_r = 1.0 TYPE 2 TO 3 FOR F_r = 1.58 NO COHERENT CORE PRESENT
D	SAME AS C BUT HIGHLY WANDERING AND UNSTEADY

SCREEN BLOCKAGE SCHEME 5

FIGURE 13 VORTEXING INSIDE SUMP; CASE 1; W.S. EL 602'-10" (MODIFIED SUMP)

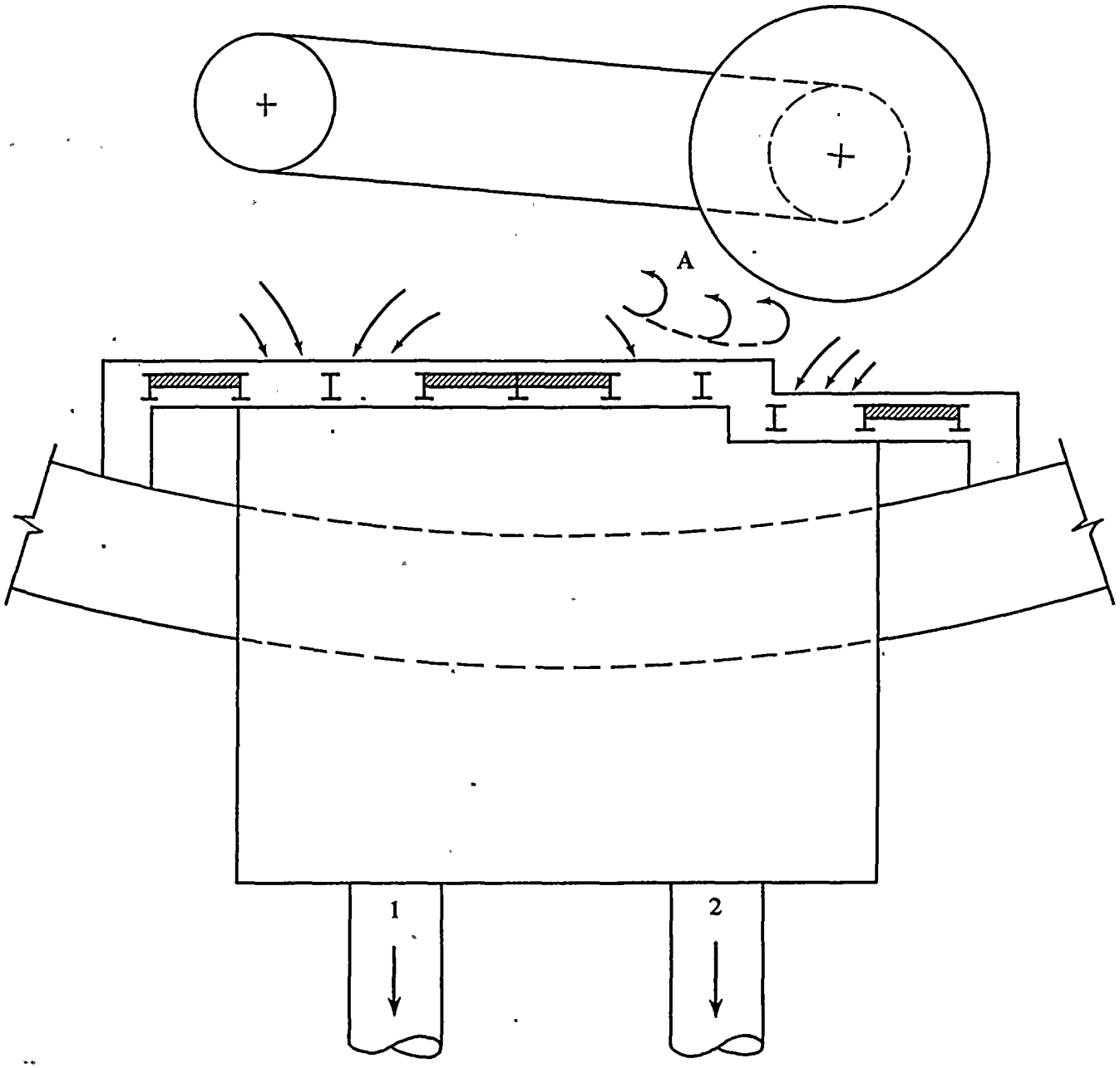

A FOR F_r = 1.0, WEAK SURFACE DIMPLES DUE TO EDDIES SHED BY PIPE.

FOR F_r = 1.58, TYPE 2-3 VORTICES WANDERING AND UNSTEADY; NO COHERENT CORE SEEN TO ENTER GRATING.

SCREEN BLOCKAGE SCHEME 5

FIGURE 14 VORTEXING INSIDE SUMP; CASE 2; W.S. EL 606' (MODIFIED SUMP)

ARL

CASE 1 PIPE 2 AT 9,500 GPM
W.S. EL 602 FT 10 INCHES
WITH GRATING BLOCKAGE SCHEME 5

NOTE: NUMBERS WITHIN BRACKETS DENOTE VORTEX TYPES

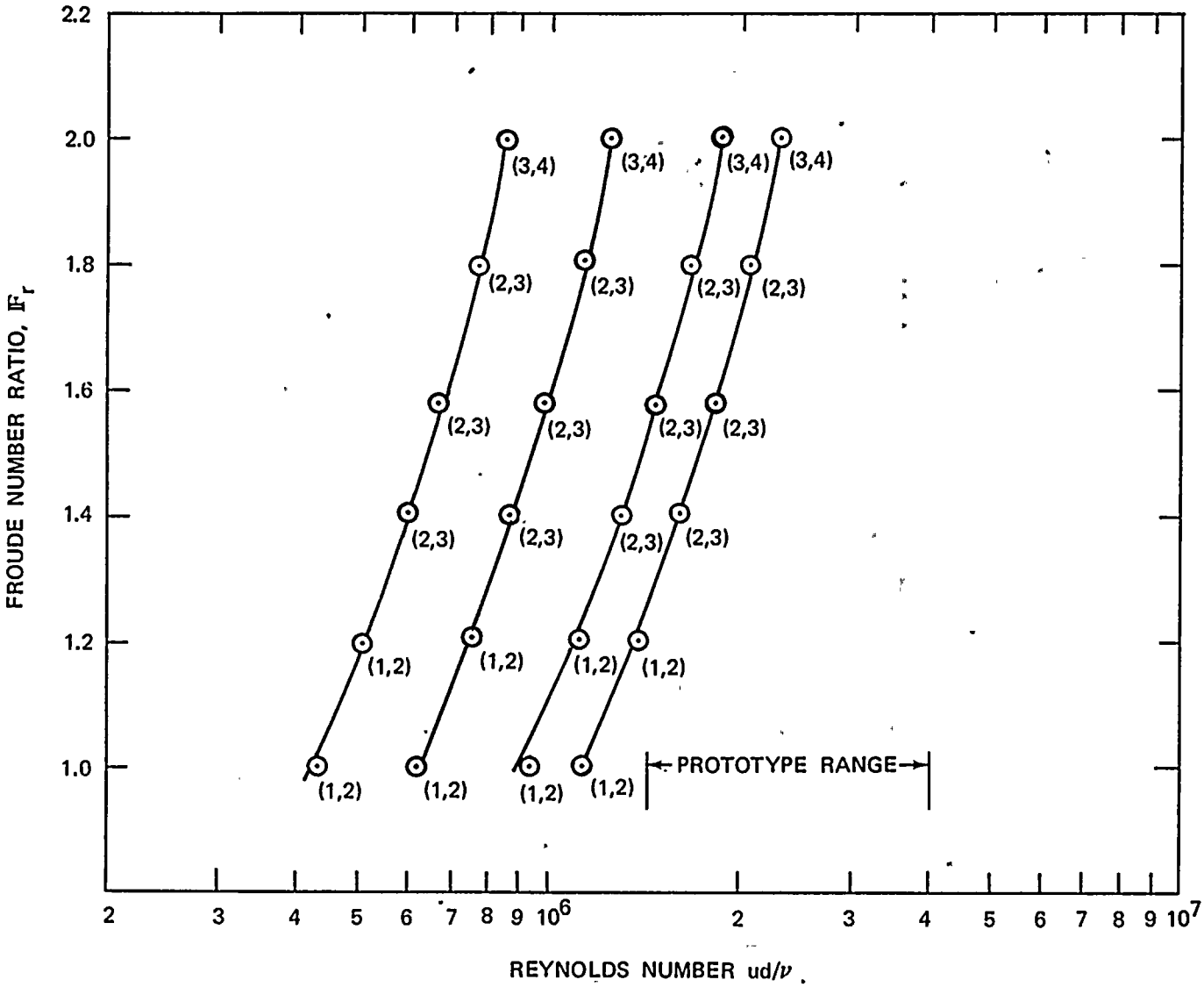

FIGURE 15 VORTEX TYPES OBSERVED DURING HIGH TEMPERATURE-HIGH VELOCITY TESTS (MODIFIED SUMP)

ARL

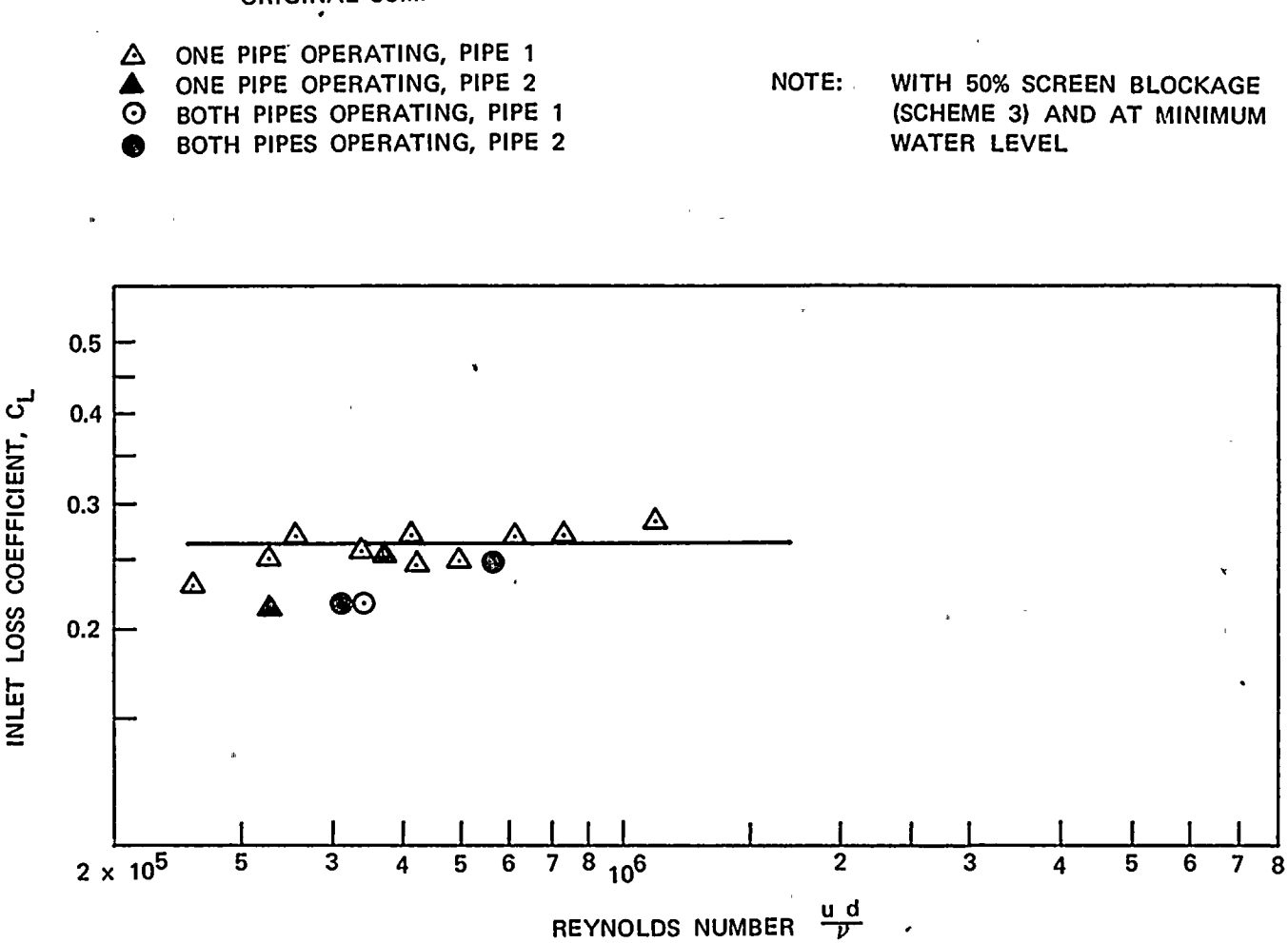

FIGURE 16 INLET LOSS COEFFICIENTS FOR ORIGINAL SUMP

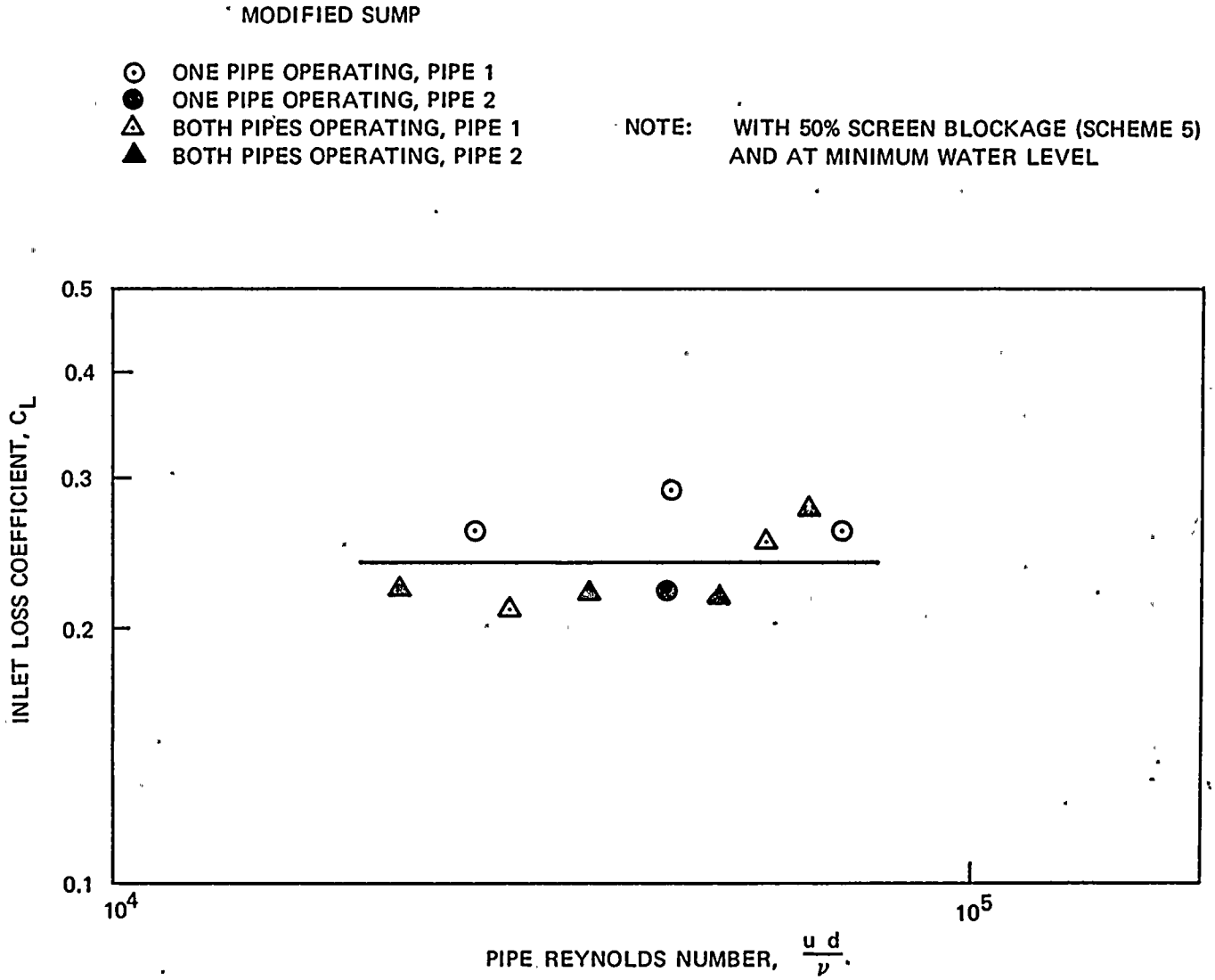

FIGURE 17 INLET LOSS COEFFICIENTS FOR MODIFIED SUMP